

# Gaussian Ensemble Belief Propagation for Efficient Inference in High-Dimensional Systems

Dan MacKinlay<sup>1</sup> Russell Tsuchida<sup>1</sup> Dan Pagendam<sup>1</sup> Petra Kuhnert<sup>1</sup>

## Abstract

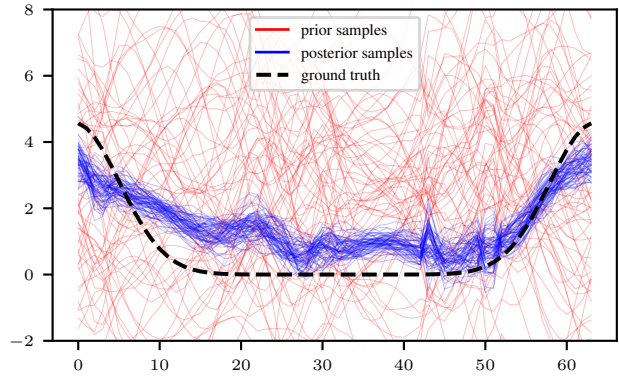
Efficient inference in high-dimensional models remains a central challenge in machine learning. This paper introduces the Gaussian Ensemble Belief Propagation (GEnBP) algorithm, a fusion of the Ensemble Kalman filter with Gaussian Belief Propagation (GaBP), which addresses this challenge by combining the strengths of both. GEnBP updates ensembles of samples from a prior distribution into samples from a posterior by passing low-rank local messages over edges in a graphical model. Ensemble techniques allow GEnBP to handle high-dimensional states, parameters and intricate, noisy, black-box generation processes. The use of local messages in a graphical model structure ensures that the approach can efficiently handle complex dependence structures. GEnBP is advantageous when the ensemble size may be considerably smaller than the inference dimension. This scenario often arises in fields such as spatiotemporal modelling, image processing and physical model inversion. GEnBP can be applied to general problem structures, including data assimilation, system identification and hierarchical models. The method is demonstrated on a range of problems, showing that it can outperform existing methods in terms of accuracy and computational efficiency.

Supporting code is available at [github.com/danmackinlay/GEnBP](https://github.com/danmackinlay/GEnBP).

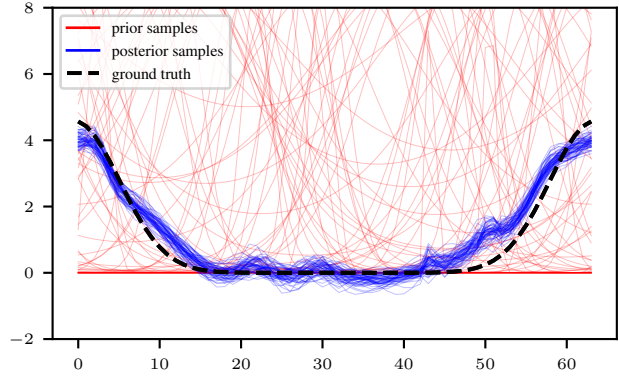
## 1. Introduction

We combine the Ensemble Kalman filter (EnKF); and Gaussian belief propagation (GaBP), to conduct inference in high-dimensional hierarchical systems. Although both these methods are well-studied, the combination appears to be powerful, simple and novel.

The EnKF (Evensen, 2003) is a popular method for inference in state space models. A posterior sample of some hidden state is constructed from prior samples by moment-



(a) GaBP  $\widehat{\text{MSE}}=1.93$ ,  $\widehat{\log p(q|\mathcal{E})}=-228$



(b) GEnBP  $\widehat{\text{MSE}}=0.167$ ,  $\widehat{\log p(q|\mathcal{E})}=-49.6$

Figure 1: Samples from the prior and posterior for the latent  $\mathbf{q}$  for the system identification problem with 1d transport dynamics (sec 4.1). The GEnBP ensemble has size  $N=64$ , and  $N=64$  samples are drawn from the GaBP beliefs.

matching the observation-conditional distribution. Although the state update may be justified in terms of a Gaussian approximation, EnKF never evaluates the Gaussian density. This trick is effective in high-dimensional problems, e.g. climate models (Houtekamer and Zhang, 2016) where the evaluation of densities can be prohibitive. However, the EnKF does not generalise beyond state-filtering.

GaBP (Yedidia et al., 2005) is a specific Gaussian message-passing algorithm for inference in graphical models. Inference is *density-based*, exploiting a nominal joint density

over the model state space. This density is approximated by a product of Gaussian factors, which define a graphical model (Koller and Friedman, 2009) over graph  $\mathcal{G}$ . Sum-product messages passed along the edges of  $\mathcal{G}$  infer some target marginal of interest (Pearl, 2008). Although the name is generic, the term GaBP is usually reserved for specific choices of message-passing and model approximation within the class of possible Gaussian message-passing algorithms (Sec. 2.2.3). Message-passing approaches are effective in many applications, including Bayesian hierarchical models (Vehtari et al., 2019; Wand, 2017), error correcting codes (Forney, 2001; Kschischang et al., 2001), and Simultaneous Locating and Mapping (SLAM) tasks (Dellaert and Kaess, 2017; Ortiz et al., 2021). Their performance may excel where the variables involved are low-dimensional. However, in high-dimensional cases, the cost of inference is typically prohibitive.

GENBP borrows strength from both methods, simultaneously attaining the efficiency of the EnKF for high-dimensional data, and GaBP’s ability to handle complex graphical model structures. GENBP can handle models with noisy and moderately non-linear observation processes, unknown process parameters, and deeply nested hierarchies of dependency between unknown variates, scaling to variables and observations with millions of dimensions. As with both GaBP and EnKF, GENBP exploits Gaussian approximations, although the statistics are given by empirical samples as in the EnKF rather than by the  $\delta$ -method as in GaBP. The class of problems amenable to this approach is practically important, encompassing many physical and geospatial systems, including computational fluid dynamics, geophysical model inversion and weather prediction. Such systems generally have a high-dimensional representation, but spatial correlations which induce a low-rank structure well captured by empirical covariance approximations.

### 1.1. Main Contributions

1. We introduce Gaussian Ensemble Belief Propagation (GENBP), a method for high-dimensional inference in graphical models with message-passing.
2. GENBP approximates Belief Propagation in Gaussian graphical models using EnKF-like ensemble statistics, rather than linearisation as in traditional GaBP.
3. GENBP scales to higher dimensions than traditional GaBP, while attaining comparable or superior accuracy in physical problems of practical import
4. GENBP is enabled by
  - (a) rank-efficient means to propagate high-dimensional Gaussian beliefs, and
  - (b) compute-efficient conversions between Gaussian beliefs and ensemble approximations,
 which are to the best of our knowledge novel in this

setting.

## 2. Preliminaries

We introduce the essential notation and concepts. Deeper background on belief propagation may be found in App. C and on the Ensemble Kalman filter in App. D.

### 2.1. Models as generative process and as density

The state space of a vector random variate written is bolded, i.e.  $\mathbf{x} \in \mathbb{R}^D$ , and the corresponding variate itself in sans-serif,  $\mathbf{x}$ . We assume that all variates possess densities, so that we may write  $\mathbf{x} \sim p(\mathbf{x})$  to assert that  $\mathbf{x}$  possesses density  $p$ .

The overall model state vector is partitioned into variables related through a structural equation model  $\mathcal{M}$  (Wright, 1934), i.e. a list of  $J$  generating equations  $\{\mathcal{P}_j\}_{1 \leq j \leq J}$ ,<sup>1</sup>

$$\mathcal{P}_j : \mathbb{R}^{D_{\mathcal{I}_j}} \rightarrow \mathbb{R}^{D_{\mathcal{O}_j}} \quad (1)$$

$$\mathbf{x}_{\mathcal{I}_j} \mapsto \mathbf{x}_{\mathcal{O}_j}. \quad (2)$$

Each  $\mathcal{P}_j$  induces a relationship between *inputs*  $\mathcal{I}_j$ , and *outputs*  $\mathcal{O}_j$ .<sup>2</sup> The *ancestral* variables  $\mathcal{A} := \bigcup_{\mathcal{I}_j = \emptyset} \mathcal{O}_j$  are those without inputs. We categorise variables as *Evidence*  $\mathcal{E}$ , which will be observed, *latent*  $\mathcal{L}$ , which are unobserved, ‘nuisance’ variables, and *query*  $\mathcal{Q}$ , whose evidence-conditional distribution is our main interest. In this work, we take the query to be the ancestral variable,  $\mathcal{Q} = \mathcal{A}$ .<sup>3</sup> Our primary target is

$$p(\mathbf{x}_{\mathcal{Q}} | \mathbf{x}_{\mathcal{E}} = \mathbf{x}_{\mathcal{E}}^*) = \frac{\int p(\mathbf{x}_{\mathcal{Q}}, \mathbf{x}_{\mathcal{L}}, \mathbf{x}_{\mathcal{E}} = \mathbf{x}_{\mathcal{E}}^*) d\mathbf{x}_{\mathcal{L}}}{\int p(\mathbf{x}_{\mathcal{Q}}, \mathbf{x}_{\mathcal{L}}, \mathbf{x}_{\mathcal{E}} = \mathbf{x}_{\mathcal{E}}^*) d\mathbf{x}_{\mathcal{Q}} d\mathbf{x}_{\mathcal{L}}}. \quad (3)$$

### 2.2. BP in graphical models

In graphical models we associate a graph structure  $\mathcal{G}$  with the factorisation of the model density and use this to calculate the target distribution (3). Readers unfamiliar with this topic should refer to App. C. We use *loopy belief propagation* (BP) in factor graphs (Kschischang et al., 2001). The factor graph is generated by writing each conditional  $j$  as a *factor potential*,  $f_j$ ,

$$p(\mathbf{x}) = \prod_j p(\mathbf{x}_{\mathcal{O}_j} | \mathbf{x}_{\mathcal{I}_j}) = \prod_j f_j(\mathbf{x}_{\mathcal{N}_j}). \quad (4)$$

where  $\mathcal{N}_j := \mathcal{O}_j \cup \mathcal{I}_j$ . The factor graph  $\mathcal{G}$  is bipartite, with a factor node  $j$  for each factor potential  $f_j(\mathbf{x}_{\mathcal{N}_j})$  and a variable node  $k$  for each variable  $\mathbf{x}_k$ . BP estimates a *belief*

<sup>1</sup>We allow each  $\mathcal{P}$  to be a stochastic function, i.e. a deterministic function  $\mathbf{x}_{\mathcal{O}_j} = \mathcal{P}_j(\mathbf{x}_{\mathcal{I}_j}, \mathbf{n}_j)$  with unobservable noise term  $\mathbf{n}_j$ . We suppress the noise terms for compactness.

<sup>2</sup>Any of these sets may be empty.

<sup>3</sup>Extending our approach to more general cases is straightforward but complicates the introduction.

over a query node,  $b_G(\mathbf{x}_\varnothing) = \int p(\mathbf{x}) d\mathbf{x}_{\setminus\varnothing}$ , by integrating out all other variates.

**Proposition 1** (Belief Propagation on Factor Graphs). *The following messages,*

$$m_{f_j \rightarrow \mathbf{x}_k} = \int \left( f_j(\mathbf{x}_{\mathcal{N}_j}) \prod_{i \in \mathcal{N}_j \setminus k} m_{\mathbf{x}_i \rightarrow f_j} \right) d\mathbf{x}_{\mathcal{N}_j \setminus k} \quad (5)$$

$$m_{\mathbf{x}_k \rightarrow f_j} = \prod_{s \in \mathcal{N}_k \setminus j} m_{f_s \rightarrow \mathbf{x}_k}, \quad (6)$$

iteratively and synchronously propagated between all the nodes in the associated factor graph, yield the approximate marginal at target variable node,

$$b_G(\mathbf{x}_k) := \prod_{s \in \mathcal{N}_k} m_{f_s \rightarrow \mathbf{x}_k} \approx \int p(\mathbf{x}) d\mathbf{x}_{\setminus k}. \quad (7)$$

The fixed points of this iteration are the fixed points of the Bethe approximation to the target marginal.

*Proof.* Yedidia et al. (2000).  $\square$

Analysis of quality of this approximation is complicated (Yedidia et al., 2005; Weiss and Freeman, 2001) but in many applications produces SOTA results (Davison and Ortiz, 2019).

### 2.2.1. THE POSTERIOR GRAPH

We have so far discussed a graph  $\mathcal{G}$  associated with the generative model prior. In practice we are more interested in the evidence-conditional posterior graph  $\mathcal{G}^*$  which encodes (3), obtained by conditioning on  $\mathbf{x}_{\mathcal{E}} = \mathbf{x}_{\mathcal{E}}^*$ . We construct  $\mathcal{G}^*$  by altering factors  $f_j, \forall j \in \mathcal{N}_{\mathcal{E}}$  in the prior graph,

$$f_j(\mathbf{x}_j) \leftarrow f_j^*(\mathbf{x}_{\mathcal{N}_j \setminus \mathcal{E}}) := p(\mathbf{x}_{\mathcal{N}_j \setminus \mathcal{E}} | \mathbf{x}_{\mathcal{E}} = \mathbf{x}_{\mathcal{E}}^*). \quad (8)$$

The target marginal is then  $p(\mathbf{x}_\varnothing | \mathbf{x}_{\mathcal{E}} = \mathbf{x}_{\mathcal{E}}^*) \approx b_{\mathcal{G}^*}(\mathbf{x}_\varnothing)$ ; see Fig 8 in the Appendix..

### 2.2.2. CONSTRUCTING A NOVEL BP METHOD

To find a target evidence-conditional marginal  $b_{\mathcal{G}^*}(\mathbf{x}_\varnothing)$  from a prior factor graph we need to be able to 1) find posterior factors by conditioning (8), and 2) calculate the BP messages of Prop. 1. We use the following set of operations defined upon factor and variable densities:

**Definition 1.** Consider the concatenated state space  $\mathbf{x}^\top = [\mathbf{x}_k^\top \quad \mathbf{x}_\ell^\top]$  at some node in a factor graph, with parametric density  $f(\mathbf{x}; \boldsymbol{\theta})$ . Sufficient operations for BP are:

**Conditioning:**

$$f(\mathbf{x}; \boldsymbol{\theta}), \mathbf{x}_k^* \mapsto f^*(\mathbf{x}_\ell; \boldsymbol{\theta}_\ell^*) =: f(\mathbf{x}_\ell | \mathbf{x}_k = \mathbf{x}_k^*); \quad (9)$$

**Marginalisation:**

$$f(\mathbf{x}; \boldsymbol{\theta}) \mapsto f(\mathbf{x}_k; \boldsymbol{\theta}_k) =: \int f(\mathbf{x}; \boldsymbol{\theta}) d\mathbf{x}_\ell; \quad (10)$$

**Multiplication:**

$$f(\mathbf{x}; \boldsymbol{\theta}), f(\mathbf{x}_k; \boldsymbol{\theta}_k) \mapsto f(\mathbf{x}; \boldsymbol{\theta}') =: f(\mathbf{x}; \boldsymbol{\theta}) f(\mathbf{x}_k; \boldsymbol{\theta}_k). \quad (11)$$

Typically such operations are implemented in terms of the  $\boldsymbol{\theta}_{(\cdot)}$  parameters of the density functions.

**Remark 1.** To calculate the marginal belief over a target variable  $\mathbf{x}_\varnothing$  by message passing in a observation-conditional factor graph (8) a sufficient set of operations defined over factors and variables is (9), (10) and (11).

### 2.2.3. GAUSSIAN DISTRIBUTIONS IN BP

If the relationships between variables are linear with additive Gaussian noise, and the ancestral distributions are Gaussian, then the density over each factor is Gaussian. Then, all of the requisite operations of Rem. 1 have closed form (Bickson, 2009; Yedidia et al., 2000), a fact exploited in classic GaBP (Dellaert and Kaess, 2017), which we introduce here. We exploit two forms for the Gaussian density. The moments-form Gaussian density is

$$\phi_M(\mathbf{x}; \mathbf{m}, K) = |2\pi K|^{-1/2} e^{-1/2(\mathbf{x}-\mathbf{m})^\top K^{-1}(\mathbf{x}-\mathbf{m})} \quad (12)$$

The canonical form

$$\phi_C(\mathbf{x}; \mathbf{n}, P) = |P/2\pi|^{1/2} e^{-\frac{\mathbf{x}^\top P \mathbf{x}}{2} + \mathbf{n}^\top \mathbf{x} - \frac{\mathbf{n}^\top P^{-1} \mathbf{n}}{2}}, \quad (13)$$

The respective parameters are with mean  $\mathbf{m}$  and covariance  $K$ ; and precision  $P = K^{-1}$  and information  $\mathbf{n} = P\mathbf{m}$ , assuming the necessary inverses exist. See details in App. C.3. The most challenging operation is multiplication (11):

$$\phi_C(\mathbf{x}; \mathbf{n}, P) \phi_C(\mathbf{x}_k; \mathbf{n}', P') \propto \phi_C(\mathbf{x}; \mathbf{n} + \mathbf{n}', P + P'). \quad (14)$$

Where the factor potentials arise from some nonlinear simulator  $\mathcal{P}$  the joint covariance is not Gaussian. Standard GaBP practice (e.g. Eustice et al., 2006; Ranganathan et al., 2007; Dellaert and Kaess, 2017) is to use propagation-of-errors, a.k.a. the  $\delta$ -method (Dorfman, 1938) to find parameters of approximating Gaussian densities. In the bivariate case where  $\mathbf{x}_2 = \mathcal{P}(\mathbf{x}_1)$ ,  $\mathbb{E}[\mathbf{x}_1] = \mathbf{m}_1$  and  $\text{Var} \mathbf{x}_1 = K_1$ , and defining where we defined  $J := \nabla_{\mathbf{x}} \mathcal{P}(\mathbf{x})|_{\mathbf{x}=\mathbf{m}_1}$ , this is

$$\begin{bmatrix} \mathbf{x}_1 \\ \mathbf{x}_2 \end{bmatrix} \stackrel{\text{approx}}{\sim} \phi_M \left( \begin{bmatrix} \mathbf{x}_1 \\ \mathbf{x}_2 \end{bmatrix}; \begin{bmatrix} \mathbf{m}_1 \\ \mathcal{P}(\mathbf{m}_1) \end{bmatrix}, K \right) \text{ where} \quad (15)$$

$$K = \begin{bmatrix} K_1 & JK_1 \\ K_1 J^\top & JK_1 J^\top \end{bmatrix}. \quad (16)$$

The accuracy of the  $\delta$ -method is complicated to analyse for nonlinear  $\mathcal{P}$  although bounds on e.g the Jensen gap (Gao et al., 2020) of the approximation are available (See App. C.4), these are rarely calculated in practice. GaBP scales unfavourably with the dimension of nodes, at memory cost  $\mathcal{O}(D^2)$  and time cost  $\mathcal{O}(D^3)$  whenever a  $D \times D$  covariance matrix is inverted.

### 2.3. Ensemble Kalman Filtering

A method which ameliorates large- $D$  costs at acceptable accuracy is EnKF. Where the GaBP method summarises inference in terms of the parameters of a Gaussian distribution, the EnKF summarises the prior distributions in terms of *ensembles* of Monte Carlo samples, i.e. a matrix of  $N$  samples,  $X := [\mathbf{x}^{(n)}]_{1 \leq n \leq N}$  drawn i.i.d. from the prior distribution,  $\mathbf{x}^{(n)} \sim \phi_M(\mathbf{x}; \mathbf{m}, \mathbf{K})$ . Introducing the matrices  $A_N := [\frac{1}{N} \ \cdots \ \frac{1}{N}]^\top$ ,  $B_N := [1 \ \cdots \ 1]$  and  $C_N := I_N - A_N B_N$ , we define

$$\bar{X} := X A_N \quad \text{Ensemble mean} \quad (17)$$

$$\check{X} := X - X A_N B_N = X C_N. \quad \text{Ensemble deviation} \quad (18)$$

We hereafter suppress  $N$ , which is uniquely determined by context. Overloading the mean and variance operations to describe empirical moment of ensembles, we write

$$\widehat{\mathbb{E}}X = \bar{X} \quad (19)$$

$$\widehat{\text{Var}}_V X = \frac{1}{N-1} \check{X} \check{X}^\top + V \quad (20)$$

$$\widehat{\text{Cov}}(X, Y) = \frac{1}{N-1} \check{X} \check{Y}^\top \quad (21)$$

$V$  is a diagonal matrix *nugget* term, typically set to  $\sigma^2 I$ . Setting  $\sigma > 0$  is useful for numerical stability, and to encode model uncertainty. Such diagonal terms are in practice algorithm hyperparameters, and also arise in GaBP. The statistics of ensemble  $X$  define an implied Gaussian density,  $\mathbf{x} \sim \phi_M(\mathbf{x}; \bar{X}, \widehat{\text{Var}}_V X)$ . The prior model ensembles are sampled by ancestral sampling with generative equations (31).

Two of the BP operations from Rem. 1 are known for the EnKF.

**Proposition 2.** Partition  $\mathbf{x} = \begin{bmatrix} \mathbf{x}_k \\ \mathbf{x}_\ell \end{bmatrix}$  so  $X = \begin{bmatrix} X_k \\ X_\ell \end{bmatrix}$ , and

$$X \sim \phi_M \left( \begin{bmatrix} \mathbf{x}_k \\ \mathbf{x}_\ell \end{bmatrix}; \begin{bmatrix} \bar{X}_k \\ \bar{X}_\ell \end{bmatrix}, \begin{bmatrix} \widehat{\text{Var}}_V X_k & \widehat{\text{Cov}}(X_k, X_\ell) \\ \widehat{\text{Cov}}(X_k, X_\ell) & \widehat{\text{Var}}_V(X_\ell) \end{bmatrix} \right). \quad (22)$$

In ensemble form, conditioning (9) becomes

$$X, \mathbf{x}_k^* \mapsto X_\ell + \widehat{\text{Cov}}(X_\ell, X_k) \widehat{\text{Var}}_V^{-1}(X_k) (\mathbf{x}_k^* - X_k) \quad (23)$$

The time cost of (23) is  $\mathcal{O}(N^3 + N^2 D_{\mathbf{x}_k})$ . Marginalisation (10) is simply truncation,  $X \mapsto X_k$ .

*Proof.* Appendix D.  $\square$

Whether the EnKF provides a good approximation to the target distribution for any  $N$  depends on the specific problem

but in many spatiotemporal systems we find good results for  $N \ll D$ , in which case the cost conditioning is superior to the  $\mathcal{O}(D_{\mathbf{x}_k}^3)$  cost of the GaBP.

Although the EnKF is motivated by a Gaussian conditional update, we note that the Gaussian approximation to the joint is different to that used in GaBP (15), which depends upon linearisation about the mean. The EnKF by contrast, samples from the full joint distribution, and so potentially reduces the Jensen gap penalty paid by the GaBP for nonlinear relationships, even while it reduces the computational cost.

The EnKF algorithm exploits the state-space model structure, iteratively updating using (23). That part does not generalise to other model structures without the density-multiplication operation (11) needed for belief propagation so is deferred to App. D. In the sequel, we show how to extend an EnKF-like approach to the BP setting by defining such operations.

### 3. Gaussian Ensemble Belief Propagation

GEnBP interleaves EnKF- and GaBP-type operations. GEnBP is to GaBP as Ensemble Kalman Filter is to the Extended Kalman Filter: both extend a method originally developed under linear assumptions to address more complex, non-linear scenarios (Fig. 10). Both use Gaussian approximations to approximate the true posterior distribution; while GaBP uses the  $\delta$ -method, GEnBP uses ensemble statistics.

GEnBP samples from the generative prior, converts the ensemble statistics to canonical form, conducts belief propagation, and then recovers ensemble samples matching the updated beliefs (Tab. 1). Although there are several steps (listed in Alg. 1), the shared strategy is to conduct the steps of a belief-propagation-type algorithm using low-rank Gaussian statistics from the EnKF approximation without ever forming a full covariance matrix.

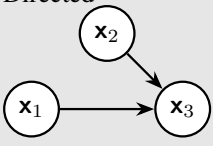
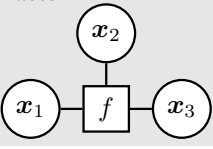
Throughout we regard an approximation  $\phi_M(\hat{\mathbf{m}}, \hat{\mathbf{K}})$  to a target Gaussian  $\phi_M(\mathbf{m}, \mathbf{K})$  to be the *best* if  $\hat{\mathbf{m}} = \mathbf{m}$  and Frobenius loss  $\|\hat{\mathbf{K}} - \mathbf{K}\|_F$  is minimised. This equates to minimising the Maximum Mean Discrepancy with the polynomial kernel of order 2 between those distributions (Sriperumbudur et al., 2010, Ex. 3).

#### 3.1. Nearly-low-rank Gaussian parameters

The GEnBP workhorse is efficient computation using the *nearly-low-rank* Gaussian moments induced by the ensemble samples. This enables translation between ensemble statistics, various parameterisations, and efficient operations upon those parameters.

**Definition 2.** A positive-definite, symmetric matrix  $\mathbf{K} \in$

Table 1: Relations in Gaussian Ensemble Belief Propagation

	Generative	Density-based
Operations	<ul style="list-style-type: none"> <li>• Sample</li> <li>• Condition</li> </ul>	<ul style="list-style-type: none"> <li>• Propagate</li> </ul>
Graph type	Directed 	Factor 
Decomposition	$\mathbf{x}_3 = \mathcal{P}(\mathbf{x}_1, \mathbf{x}_2)$	$f(x_1, x_2, x_3)$
Node Parameters	Empirical moments $\mathbf{m}, \mathbf{K}$	Canonical parameters $\mathbf{n}, \mathbf{P}$

↖ Empirical statistics  
↙ Ensemble recovery

**Algorithm 1** GENBP

**Require:** Graph  $\mathcal{G}$ , set of generative processes  $\{\mathcal{P}_j\}_j$ , observations  $\mathbf{x}_{\mathcal{O}}$ , ancestral sample  $X_{\mathcal{A}}$ .

**Ensure:** Observation-conditional sample  $X_{\mathcal{O}}^*$ .

- 1: **while** not converged **do**
- 2: Sample ensemble from the generative processes  $\mathcal{P}_j$  on  $\mathcal{G}$  using (4)
- 3: Convert  $\mathcal{G}$  into the conditional graph  $\mathcal{G}^*$  by conditioning observed factors (8) using (23)
- 4: Convert variables and factors to nearly-low-rank canonical form {Sec. 3.1}
- 5: Propagate nearly-low-rank messages on  $\mathcal{G}^*$  {Sec. 3.3/Alg. 2}
- 6: Conform ancestral nodes to belief  $T(X_{\mathcal{O}}^*) \sim b_{\mathcal{G}^*}(\mathbf{x}_{\mathcal{A}})$  {Sec. 3.4}
- 7: **end while**
- 8: Return Approximate posterior sample  $X_{\mathcal{O}}^*$ .

$\mathbb{R}^{D \times D}$  is nearly-low-rank if  $\mathbf{K} = \mathbf{V} \pm \mathbf{L}\mathbf{L}^\top$  where  $\mathbf{L} \in \mathbb{R}^{D \times N}$  is a low rank component matrix with  $N \ll D$  and  $\mathbf{V} = \text{diag}(\mathbf{v})$  is a  $D \times D$  diagonal matrix. Properties of such matrices are expanded in App. F.

The empirical variance in the EnKF (20) is nearly-low-rank with component  $\mathbf{L} = \tilde{\mathbf{X}}/\sqrt{N-1}$  and diagonal  $\mathbf{V} = \sigma^2\mathbf{I}$ . We initialise the belief-propagation stage of the algorithm (step 1), setting the distribution for each factor  $f_j^*$  to the empirical distribution of the ensemble at that factor,  $X_j$ ,

$$f_j^* \sim \phi_M(\mathbf{x}; \bar{X}_j, \widehat{\text{Var}}_{\gamma^2\mathbf{I}}X). \quad (24)$$

**Proposition 3.** Suppose  $\mathbf{x} \sim \phi_M(\cdot; \mathbf{m}, \mathbf{K})$  has nearly-low-rank variance  $\mathbf{K} = \mathbf{L}\mathbf{L}^\top + \mathbf{V}$ ,  $\mathbf{L} \in \mathbb{R}^{D \times N}$ . We may find the parameters of that density in canonical form  $\phi_C(\cdot; \mathbf{n}, \mathbf{P})$

as  $\mathbf{n} = \mathbf{P}\mathbf{m}$  and precision  $\mathbf{P} = \mathbf{K}^{-1} = \mathbf{U} - \mathbf{R}\mathbf{R}^\top$ , at a time cost of  $\mathcal{O}(N^3 + N^2D)$ . Further, we may recover the moments-form from the canonical at the same cost.

*Proof.* Appendix F.3 □

### 3.2. Nearly-low-rank belief propagation

Density multiplication (14) is simple in the nearly-low-rank representation.

**Proposition 4.** Suppose we are given two canonical-form Gaussian densities with respective information and precisions  $\mathbf{n}', \mathbf{P}'$  and  $\mathbf{n}'', \mathbf{P}''$ , where the precisions are both nearly low rank,  $\mathbf{P}' = \mathbf{U}' - \mathbf{R}'\mathbf{R}'^\top$  and  $\mathbf{P}'' = \mathbf{U}'' - \mathbf{R}''\mathbf{R}''^\top$  where  $\mathbf{R}' \in \mathbb{R}^{D \times N'}$  and  $\mathbf{R}'' \in \mathbb{R}^{D \times N''}$  and  $\mathbf{U}', \mathbf{U}''$  diagonal. Then the parameters  $\mathbf{n}, \mathbf{P}$  of the multiplied density  $\phi_C(\cdot; \mathbf{n}, \mathbf{P}) = \phi_C(\cdot; \mathbf{n}', \mathbf{P}')\phi_C(\cdot; \mathbf{n}'', \mathbf{P}'')$  are given by

$$\mathbf{n} = \mathbf{n}' + \mathbf{n}'' \text{ and} \quad (25)$$

$$\mathbf{P} = \mathbf{P}' + \mathbf{P}'' = \mathbf{U} - \mathbf{R}\mathbf{R}^\top, \text{ where} \quad (26)$$

$$\mathbf{U} = \mathbf{U}' + \mathbf{U}'', \text{ and } \mathbf{R} = [\mathbf{R}' \quad \mathbf{R}''] \quad (27)$$

$\mathbf{P}$  is also nearly-low-rank, with  $\mathbf{R} \in \mathbb{R}^{D \times (N' + N'')}$ .

*Proof.* Follows from (44) and (81) in the appendix. □

### 3.3. GENBP messages

The most complicated and costly step is the factor-to-variable message (5),  $f_j \rightarrow \mathbf{x}_k$ , which is detailed in Alg. 2 for a single incoming message  $\mathbf{x}_\ell \rightarrow f_j$ . Generalisation to multiple incoming messages is by iterative application of the algorithm. Variable-to-factor messages are a degenerate case.

**Algorithm 2** GEnBP  $f_j \rightarrow \mathbf{x}_k$  factor-to-variable message with a single incoming message  $\mathbf{x}_\ell \rightarrow f_j$ .

**Require:** Gaussian factor canonical parameters for  $f_j$ ,  $\mathbf{n} =$

$$\begin{bmatrix} \mathbf{n}_\ell \\ \mathbf{n}_k \end{bmatrix}, \mathbf{P} = \mathbf{U} - \begin{bmatrix} \mathbf{R}_\ell \\ \mathbf{R}_k \end{bmatrix} \begin{bmatrix} \mathbf{R}_\ell \\ \mathbf{R}_k \end{bmatrix}^\top \text{ for } \mathbf{U} = \text{diag} \left( \begin{bmatrix} \mathbf{u}_\ell \\ \mathbf{u}_k \end{bmatrix} \right)$$

with  $\mathbf{R}_\ell \in \mathbb{R}^{D_\ell \times N}$ ,  $\mathbf{R}_k \in \mathbb{R}^{D_k \times N}$

**Require:**  $\mathbf{x}_k \rightarrow f_j$  Gaussian message parameters  $\mathbf{n}'_k \in \mathbb{R}^{D_k}$  and precision  $\mathbf{P}_k = \mathbf{U}'_k - \mathbf{R}'_k \mathbf{R}'_k{}^\top$ ,  $\mathbf{R}'_k \in \mathbb{R}^{D_k \times N'}$  and  $\mathbf{U}' = \text{diag}(\mathbf{u}'_k)$

**Ensure:**  $f_j \rightarrow \mathbf{x}_\ell$  Gaussian message parameters  $\mathbf{n}'_\ell$ ,  $\mathbf{P}'_\ell = \mathbf{U}'_\ell - \mathbf{R}'_\ell \mathbf{R}'_\ell{}^\top$

- 1: Joint information vector  $\mathbf{n}_\Pi^\top \leftarrow [\mathbf{n}_\ell^\top \quad (\mathbf{n}_k + \mathbf{n}'_k)^\top]$ .
- 2: Joint precision  $\mathbf{P}_\Pi \leftarrow \mathbf{U}_\Pi - \mathbf{R}_\Pi \mathbf{R}_\Pi^\top$ ,  $\mathbf{R}_\Pi = \begin{bmatrix} \mathbf{R}_\ell & 0 \\ \mathbf{R}_k & \mathbf{R}'_k \end{bmatrix}$ ,  $\mathbf{U}_\Pi = \text{diag} \left( \begin{bmatrix} \mathbf{u}_\ell \\ \mathbf{u}_k + \mathbf{u}'_k \end{bmatrix} \right)$
- 3: Joint covariance  $\mathbf{K}_\Pi \leftarrow \mathbf{P}_\Pi^{-1} = \mathbf{V}_\Pi + \mathbf{L}_\Pi \mathbf{L}_\Pi^\top$  where  $\mathbf{L}_\Pi \in \mathbb{R}^{(D_k + D_\ell) \times (N + N')}$ ,  $\mathbf{V}_\Pi = \text{diag}(\mathbf{v}_\Pi)$
- 4: Calculate joint mean  $\mathbf{m}_\Pi = \mathbf{P}_\Pi \mathbf{n}_\Pi$
- 5: Form the marginal mean over  $\mathbf{x}_\ell$ ,  $\mathbf{m}_\ell = \mathbf{m}_\Pi[1:D_k]$
- 6: Form the marginal covariance over  $\mathbf{x}_\ell$ ,  $\mathbf{K}_\ell = \mathbf{V}_\ell + \mathbf{L}_\ell \mathbf{L}_\ell^\top$  where  $\mathbf{L}_\Pi[1:D_k, 1:(N' + N)]$ ,  $\mathbf{V}_\ell = \text{diag}(\mathbf{v}_\Pi[1:D_k])$
- 7: Constrain the rank of  $\mathbf{K}_\ell \leftarrow \mathbf{K}'_\ell = \mathbf{V}_\ell + \mathbf{L}'_\ell \mathbf{L}'_\ell{}^\top$  to  $N$  setting  $\mathbf{L}'_\ell = \mathbf{A}\mathbf{S}$  for  $\mathbf{A}$  the left singular vectors and  $\mathbf{S}$  the top  $n$  singular values
- 8: Calculate the marginal precision  $\mathbf{P}'_\ell = \mathbf{K}'_\ell^{-1} = \mathbf{U}_\ell - \mathbf{R}_\ell \mathbf{R}_\ell^\top$
- 9: Calculate the marginal information vector  $\mathbf{n}'_\ell = \mathbf{P}'_\ell \mathbf{m}_\ell$
- 10: Return canonical information vector  $\mathbf{n}'_\ell$
- 11: Return canonical precision  $\mathbf{P}'_\ell$

Suppose we wish to calculate an outgoing message from  $D$ -dimensional factor  $f$ , with  $K$  neighbours, to a  $d$ -dimensional variable node. In the worst case, messages are incoming from  $K - 1$  neighbours, so the concatenated components of the factor belief precision matrix in step 2 form a  $D \times NK$  matrix. Inverting this (step 2) costs  $\mathcal{O}(DN^2K^2 + N^3K^3)$  (Prop 8). We discover a size- $N$  basis using SVD via F.5 at a cost of  $\mathcal{O}(DNK \log N + N^2(D + NK))$ . Marginalising is by truncating to the  $d$  dimensions spanned by the variable node, yielding  $d \times N$  variance component matrices. The canonical form of the reduced-rank belief may be found with time cost of  $\mathcal{O}(N^3 + N^2d)$  using 9, at an overall cost of  $\mathcal{O}(DN^2K^2 + N^3K^3)$ .

### 3.4. Nearly-low-rank ensemble conformation

The final step of the GEnBP algorithm is *ensemble conformation*, which transforms a prior ensemble into a posterior ensemble whose statistics are maximally consistent with the posterior belief  $b_{\mathcal{G}^*}(\mathbf{x}_\mathcal{Q}) = \phi_M(\mathbf{x}_\mathcal{Q}; \mathbf{m}_\mathcal{Q}, \mathbf{K}_\mathcal{Q})$  at query node  $\mathcal{Q}$ , i.e.  $T(X) \stackrel{\text{approx}}{\sim} b_{\mathcal{G}^*}$ . We suppress the  $\mathcal{Q}$  subscript hereafter. Restricting ourselves to af-

fine transformations  $T_{\boldsymbol{\mu}, \mathbf{T}} : X \mapsto \boldsymbol{\mu}\mathbf{B} + \check{\mathbf{X}}\mathbf{T}$  leaves the parameters  $\boldsymbol{\mu} \in \mathbb{R}^D$ ,  $\mathbf{T} \in \mathbb{R}^{M \times M}$  to be chosen. Fixing  $\boldsymbol{\mu} \equiv \mathbf{m}$ , we choose  $\mathbf{T}$  to optimise the Frobenius distance between the variances of the mapped ensemble and the target  $\mathbf{K} = \mathbf{L}\mathbf{L}^\top + \mathbf{V}$ , with  $\mathbf{V}$  diagonal,

$$\mathbf{T} := \text{argmin}_{\mathbf{T}^*} \left\| \widehat{\text{Var}}_{\eta^2 \mathbf{I}}(\boldsymbol{\mu}\mathbf{B} + \check{\mathbf{X}}\mathbf{T}^*) - \mathbf{K} \right\|_F^2 \quad (28)$$

$\mathbf{T}$  is identifiable only up to a unitary transform. We therefore find  $\mathbf{M} := \mathbf{T}\mathbf{T}^\top$  from the space of positive definite matrices, selecting a  $\mathbf{T}$  from  $\mathbf{M}$  by factorisation.

**Proposition 5.** Any symmetric positive semi-definite matrix  $\mathbf{M} = \mathbf{T}\mathbf{T}^\top$  which satisfies

$$\check{\mathbf{X}}^\top \check{\mathbf{X}} \mathbf{M} \check{\mathbf{X}}^\top \check{\mathbf{X}} = (N-1) \left( \check{\mathbf{X}}^\top \mathbf{L} (\check{\mathbf{X}}^\top \mathbf{L})^\top - \check{\mathbf{X}}^\top (\mathbf{V} - \eta^2 \mathbf{I}) \check{\mathbf{X}} \right).$$

defines an affine transform which minimises (28). Such an  $\mathbf{M}$  may be found with memory complexity  $\mathcal{O}(M^2 + N^2)$  and time complexity  $\mathcal{O}(N^3 + DN^2 + DM^2)$  without forming  $\mathbf{K} \in \mathbb{R}^{D \times D}$ .

*Proof.* Appendix H □

For a variable with  $K$  neighbours, the worst case is  $M = KN$  so the cost comes to  $\mathcal{O}(N^3 + DN^2K^2)$ . The cost of finding the target covariance from the belief precision is  $\mathcal{O}(M^3 + DM^2) = \mathcal{O}(K^3N^3 + DK^2N^2)$  by (87), so our total cost for ensemble recovery is  $\mathcal{O}(K^3N^3 + DN^2K^2)$ .

### 3.5. Total computational cost

The total computational cost of the GEnBP algorithm depends upon graph structure and the various tuning parameters. The size of the ensemble in GEnBP is a free parameter controlling the fidelity of the approximation to classical GaBP. Empirically, in many useful problems  $N \ll D$  (App. B.2), in which case GEnBP is large- $D$  asymptotically favourable for any fixed factor degree  $K$ . Detailed costs are collated in Tab. 2 in App. I.

GEnBP is not favourable in  $K$ , scaling as  $\mathcal{O}(K^3)$  for some operations. In practice, we can reduce the size of large factor nodes by decomposing them into a chain of nodes with lower degree, the *Forney* factorisation (Forney, 2001). This modification controls  $K$  without altering models' marginal distributions (de Vries and Friston, 2017). In the system identification experiment,  $K$  may be large, since the latent parameter influences every timestep so has many neighbours, but the Forney representation caps  $K \leq 4$ . The net impact depends upon the graphical structure, but in our experiments, the cost of the additional messages is outweighed by the reduction in their cost.

## 4. Experiments

We compared GEnBP against GaBP in two synthetic randomised benchmarks. In both, the graph structure is a sys-

tem identification task (Appendix A.1), where a static parameter of interest influences a noisily observed, nonlinear dynamical system. For  $t = 1, 2, \dots, T$  we define

$$\mathbf{x}_t = \mathcal{P}_x(\mathbf{x}_{t-1}, \mathbf{q}), \quad \mathbf{y}_t = \mathcal{P}_y(\mathbf{x}_t) \quad (29)$$

where evidence is  $\mathcal{E} = \{\mathbf{y}_t = \mathbf{y}_t^*\}_{1 \leq t \leq T}$  and the query is  $\mathcal{Q} = \mathbf{q}$ .<sup>4</sup>

The GaBP implementation is modified from Ortiz et al. (2021) to allow arbitrary prior covariance. Hyperparameters are not directly comparable between the methods. We ameliorate this by choosing favourable values for each algorithm. We measure performance by mean squared error (MSE) of the posterior mean estimate  $\mathbb{E}b_{\mathcal{G}^*}(\mathbf{q}) - q_0$  and the log-likelihood  $\log b_{\mathcal{G}^*}(q_0; \mathbf{q})$  at ground truth  $q_0$ . Additional experiments and details are in App B.

#### 4.1. 1d transport model

The *transport* problem is a simple, 1d nonlinear dynamical system chosen for ease of visualisation (App. A.2). States are subject to both transport and diffusion, where the transport term introduces nonlinearity. Observations are subsampled state vectors perturbed by additive Gaussian noise. Fig. 1 shows samples from the prior and posterior distributions. GENBP estimates are substantially more accurate in terms of both posterior likelihood and MSE, as can be seen in the tighter clustering of the posterior samples about ground-truth.

#### 4.2. 2d fluid dynamics model

In the computational fluid dynamics (CFD) problem (Appendix A.3), states are governed by discretised Navier-Stokes equations over a 2d spatial domain. The parameter of interest is a static, latent forcing field  $\mathbf{q}$ . In our 2d incompressible equations the state field and forcing fields are scalar fields over a  $d \times d$  spatial domain; we stack them into vectors so that  $D_{\mathcal{Q}} = D_{\mathbf{x}_t} = d^2$ .

Fig 2 demonstrates that GENBP attaining superior accuracy, and posterior likelihood to GaBP, while scaling to a far higher  $D_{\mathcal{Q}}$ . Note the GaBP experiments are truncated because experiments with  $D_{\mathcal{Q}} > 1024$  failed to complete due to resource exhaustion. We caution against interpreting the run time of the algorithm too literally. The high-dimensional jacobian calculation in the GaBP algorithm is not parallelised effectively by the Pytorch library, which penalises that algorithm. On the other hand, optimal calculation of high-dimensional jacobian matrices can be costly, in the worst case  $\mathcal{O}(D)$  (Margossian, 2019), so avoiding them in the GENBP may be an advantage to the practitioner both in speed and in implementation burden.

<sup>4</sup>If  $\mathbf{q}$  were known, estimating  $\{\mathbf{x}_t\}_t$  from  $\{\mathbf{y}_t\}_t$  would be a filtering problem, soluble by EnKF.

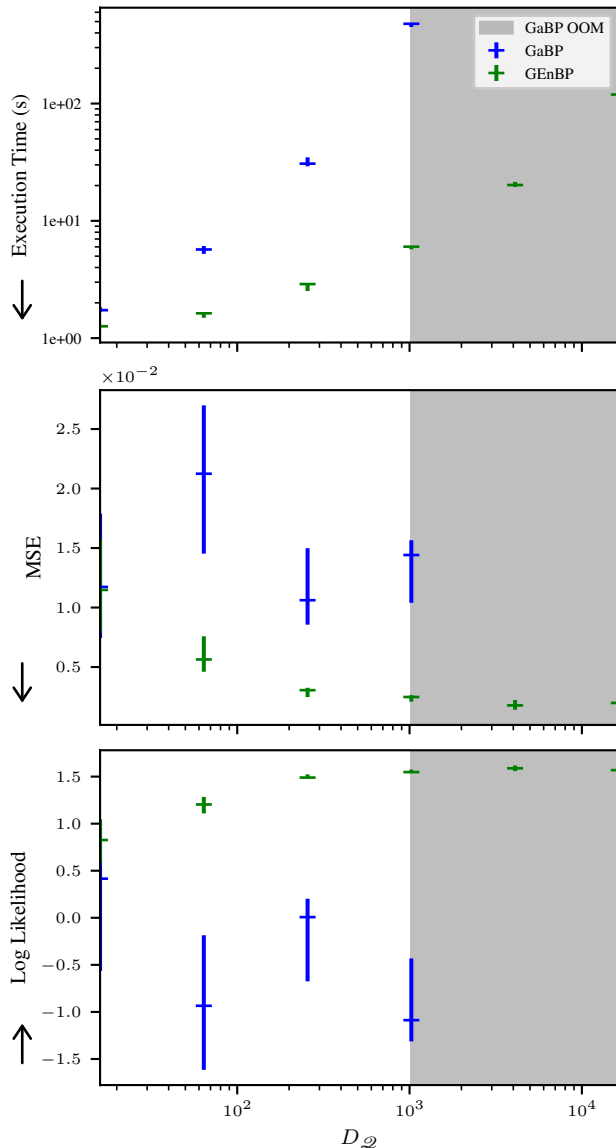


Figure 2: Influence of dimension  $D_{\mathcal{Q}}$ . Error bars show empirical 50% intervals from  $n = 10$  independent runs.

Fig 3 show the influence of the viscosity parameter  $\nu$  as it varies from laminar to turbulent flow regimes, producing diverse nonlinear behaviours (See Fig. 5). GENBP still strictly dominates GaBP in speed. It generally dominates in MSE, although there are ranges where the performance is indistinguishable or slightly worse. Regarding posterior log-likelihood of the ground-truth, GENBP is superior in the low- $\nu$  (turbulent) regime, whereas GaBP is dominant in the high- $\nu$  (laminar) regime.

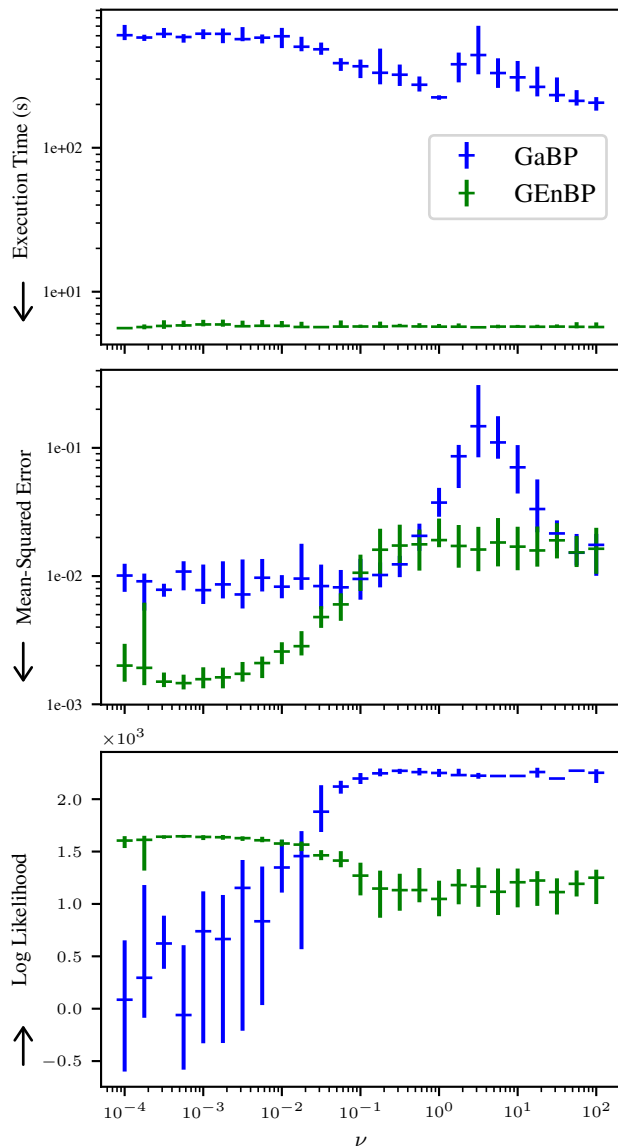


Figure 3: Influence of viscosity  $\nu$  on inference. Error bars show empirical 50% intervals from  $n = 40$  independent runs.

## 5. Conclusions

GEnBP advances the frontier of feasible inference in probabilistic graphical models. It scales to higher factor dimension than GaBP, achieving superior accuracy in some problems of interest. By employing ensemble approximations, GEnBP can accommodate the larger, more complex factors, needed in a many real-world problems. Unlike EnKF, which would be traditionally used for high dimensional systems, GEnBP can more handle intricate dependencies. It does not need gradients, and yet frequently surpasses the performance of GaBP, which does.

There are limitations to GEnBP. First, GEnBP introduces the burden of additional tuning parameters. GEnBP requires an increased number of model executions in the sampling stage, although we note that the cost of high dimensional jacobian calculations, as used in GaBP, can in practice be worse. As with EnKF, we can only expect GEnBP to be effective in systems where the underlying dynamics are nearly-low rank, i.e. where the system can be well-approximated in some low-dimensional subspace. Finally, just as the GaBP and EnKF, GEnBP still exploits Gaussian approximations and thus is also constrained to unimodal distributions. Just as with these competing methods, analysis of the convergence of GEnBP is an open question. Despite these limitations, its scalability, flexibility and ease of use makes it a promising tool for a broad range of applications, notably geospatial predictions.

Both the GaBP and EnKF literature contain improvements that we look forward to integrating into GEnBP in further work, e.g. graph pruning for improved computational efficiency (Eustice et al., 2006) or handling outliers using robust distributions (Agarwal et al., 2013). There are also other generalisations of GaBP, such as particle- (Ihler and McAllester, 2009) or Stein- (Zhuo et al., 2018) message-passing algorithms, which do not have publicly available implementations, and whose connection to GEnBP thus remains to be explored.

This work has no known wider negative societal implications other than the standard consequences of improved generic inference.

## 6. Acknowledgements

We are indebted to Laurence Davies and Hadi Afshar for helpful discussions and feedback on this work.

## References

- Pratik Agarwal, Gian Diego Tipaldi, Luciano Spinello, Cyrill Stachniss, and Wolfram Burgard. Robust map optimization using dynamic covariance scaling. In *2013 IEEE International Conference on Robotics and Automation*, pages 62–69, May 2013. doi: 10.1109/ICRA.2013.6630557.
- Danny Bickson. *Gaussian Belief Propagation: Theory and Application*. PhD thesis, July 2009.
- Andrew J. Davison and Joseph Ortiz. FutureMapping 2: Gaussian Belief Propagation for Spatial AI. *arXiv:1910.14139 [cs]*, October 2019.
- Bert de Vries and Karl J. Friston. A Factor Graph Description of Deep Temporal Active Inference. *Frontiers in Computational Neuroscience*, 11, 2017.

- Frank Dellaert and Michael Kaess. Factor Graphs for Robot Perception. *Foundations and Trends® in Robotics*, 6(1-2): 1–139, August 2017. doi: 10.1561/23000000043.
- R. A. Dorfman. A note on the  $\delta$ -method for finding variance formulae. *Biometric Bulletin*, 1938.
- Arnaud Doucet. A Note on Efficient Conditional Simulation of Gaussian Distributions. Technical report, University of British Columbia, 2010.
- Ryan M. Eustice, Hanumant Singh, and John J. Leonard. Exactly Sparse Delayed-State Filters for View-Based SLAM. *IEEE Transactions on Robotics*, 22(6):1100–1114, December 2006. doi: 10.1109/TRO.2006.886264.
- Geir Evensen. The Ensemble Kalman Filter: Theoretical formulation and practical implementation. *Ocean Dynamics*, 53(4):343–367, November 2003. doi: 10.1007/s10236-003-0036-9.
- Geir Evensen. *Data Assimilation - The Ensemble Kalman Filter*. Springer, Berlin; Heidelberg, 2009. ISBN 978-3-642-03711-5 3-642-03711-9. doi: 10.1007/978-3-642-03711-5.
- Joel H. Ferziger, Milovan Perić, and Robert L. Street. *Computational Methods for Fluid Dynamics*. Springer, Cham, 4th ed. 2020 edition edition, August 2019. ISBN 978-3-319-99691-2.
- G.D. Forney. Codes on graphs: Normal realizations. *IEEE Transactions on Information Theory*, 47(2):520–548, February 2001. doi: 10.1109/18.910573.
- Brendan J. Frey, Frank R. Kschischang, Hans-Andrea Loeliger, and Niclas Wiberg. Factor graphs and algorithms. In *Proceedings of the Annual Allerton Conference on Communication Control and Computing*, volume 35, pages 666–680. Citeseer, 1997.
- R. Furrer and T. Bengtsson. Estimation of high-dimensional prior and posterior covariance matrices in Kalman filter variants. *Journal of Multivariate Analysis*, 98(2):227–255, February 2007. doi: 10.1016/j.jmva.2006.08.003.
- Xiang Gao, Meera Sitharam, and Adrian E. Roitberg. Bounds on the Jensen Gap, and Implications for Mean-Concentrated Distributions, August 2020.
- Nathan Halko, Per-Gunnar Martinsson, and Joel A. Tropp. Finding structure with randomness: Probabilistic algorithms for constructing approximate matrix decompositions, December 2010.
- P. L. Houtekamer and Fuqing Zhang. Review of the Ensemble Kalman Filter for Atmospheric Data Assimilation. *Monthly Weather Review*, 144(12):4489–4532, December 2016. doi: 10.1175/MWR-D-15-0440.1.
- Alexander Ihler and David McAllester. Particle Belief Propagation. In *Proceedings of the Twelfth International Conference on Artificial Intelligence and Statistics*, pages 256–263. PMLR, April 2009.
- D. T. B. Kelly, K. J. H. Law, and A. M. Stuart. Well-posedness and accuracy of the ensemble Kalman filter in discrete and continuous time. *Nonlinearity*, 27(10):2579, September 2014. doi: 10.1088/0951-7715/27/10/2579.
- Daphne Koller and Nir Friedman. *Probabilistic Graphical Models : Principles and Techniques*. MIT Press, Cambridge, MA, 2009. ISBN 0-262-01319-3.
- Frank R Kschischang, Brendan J Frey, and Hans-Andrea Loeliger. Factor graphs and the sum-product algorithm. *IEEE Transactions on Information Theory*, 47(2):498–519, February 2001. doi: 10.1109/18.910572.
- Soeren Laue, Matthias Mitterreiter, and Joachim Giesen. Computing Higher Order Derivatives of Matrix and Tensor Expressions. In S. Bengio, H. Wallach, H. Larochelle, K. Grauman, N. Cesa-Bianchi, and R. Garnett, editors, *Advances in Neural Information Processing Systems 31*, pages 2750–2759. Curran Associates, Inc., 2018.
- Sören Laue, Matthias Mitterreiter, and Joachim Giesen. A simple and efficient tensor calculus. In *AAAI Conference on Artificial Intelligence, (AAAI)*. 2020.
- François Le Gland, Valérie Monbet, and Vu-Duc Tran. *Large Sample Asymptotics for the Ensemble Kalman Filter*. Report, INRIA, 2009.
- Zongyi Li, Nikola Kovachki, Kamyar Azizzadenesheli, Burigede Liu, Kaushik Bhattacharya, Andrew Stuart, and Anima Anandkumar. Fourier Neural Operator for Parametric Partial Differential Equations. *arXiv:2010.08895 [cs, math]*, October 2020.
- Charles C. Margossian. A Review of automatic differentiation and its efficient implementation. *WIREs Data Mining and Knowledge Discovery*, 9(4):e1305, July 2019. doi: 10.1002/WIDM.1305.
- Kevin P. Murphy, Yair Weiss, and Michael I. Jordan. Loopy belief propagation for approximate inference: An empirical study. In *Proceedings of the Fifteenth Conference on Uncertainty in Artificial Intelligence, UAI’99*, pages 467–475, San Francisco, CA, USA, July 1999. Morgan Kaufmann Publishers Inc. ISBN 978-1-55860-614-2.
- Joseph Ortiz, Talfan Evans, and Andrew J. Davison. A visual introduction to Gaussian Belief Propagation. *arXiv:2107.02308 [cs]*, July 2021.

- Judea Pearl. *Probabilistic Reasoning in Intelligent Systems: Networks of Plausible Inference*. The Morgan Kaufmann Series in Representation and Reasoning. Kaufmann, San Francisco, Calif, rev. 2. print., 12. [dr.] edition, 2008. ISBN 978-1-55860-479-7.
- Kaare Brandt Petersen and Michael Syskind Pedersen. The Matrix Cookbook. Technical report, 2012.
- Ananth Ranganathan, Michael Kaess, and Frank Dellaert. Loopy SAM. In *Proceedings of the 20th International Joint Conference on Artificial Intelligence, IJCAI'07*, pages 2191–2196, San Francisco, CA, USA, January 2007. Morgan Kaufmann Publishers Inc.
- Bharath K. Sriperumbudur, Arthur Gretton, Kenji Fukumizu, Bernhard Schölkopf, and Gert R. G. Lanckriet. Hilbert Space Embeddings and Metrics on Probability Measures. *Journal of Machine Learning Research*, 11:1517–1561, April 2010.
- Aki Vehtari, Andrew Gelman, Tuomas Sivula, Pasi Jylänki, Dustin Tran, Swupnil Sahai, Paul Blomstedt, John P. Cunningham, David Schiminovich, and Christian Robert. Expectation propagation as a way of life: A framework for Bayesian inference on partitioned data. *arXiv:1412.4869 [stat]*, November 2019.
- Martin J. Wainwright and Michael I. Jordan. *Graphical Models, Exponential Families, and Variational Inference*, volume 1 of *Foundations and Trends® in Machine Learning*. Now Publishers, 2008. doi: 10.1561/22000000001.
- M. P. Wand. Fast Approximate Inference for Arbitrarily Large Semiparametric Regression Models via Message Passing. *Journal of the American Statistical Association*, 112(517):137–168, January 2017. doi: 10.1080/01621459.2016.1197833.
- Yair Weiss and William T. Freeman. Correctness of Belief Propagation in Gaussian Graphical Models of Arbitrary Topology. *Neural Computation*, 13(10):2173–2200, October 2001. doi: 10.1162/089976601750541769.
- James T Wilson, Viacheslav Borovitskiy, Alexander Terenin, Peter Mostowsky, and Marc Peter Deisenroth. Pathwise Conditioning of Gaussian Processes. *Journal of Machine Learning Research*, 22(105):1–47, 2021.
- Sewall Wright. The Method of Path Coefficients. *The Annals of Mathematical Statistics*, 5(3):161–215, September 1934. doi: 10.1214/aoms/1177732676.
- Jonathan S. Yedidia, William T. Freeman, and Yair Weiss. Generalized belief propagation. In *Proceedings of the 13th International Conference on Neural Information Processing Systems, NIPS'00*, pages 668–674, Cambridge, MA, USA, January 2000. MIT Press.
- J.S. Yedidia, W.T. Freeman, and Y. Weiss. Constructing Free-Energy Approximations and Generalized Belief Propagation Algorithms. *IEEE Transactions on Information Theory*, 51(7):2282–2312, July 2005. doi: 10.1109/TIT.2005.850085.
- Jingwei Zhuo, Chang Liu, Jiaxin Shi, Jun Zhu, Ning Chen, and Bo Zhang. Message Passing Stein Variational Gradient Descent. In *Proceedings of the 35th International Conference on Machine Learning*, pages 6018–6027. PMLR, July 2018.

## A. Benchmark problems

To demonstrate the utility of our method, we select example problems of system identification type, where a latent parameter of interest must be inferred from its effects upon the dynamics of a hidden Markov model. As such it is closely related to, but more challenging than, state filtering.

Throughout, unless otherwise specified, the hyper parameters of the algorithms are  $\gamma^2 = 0.01$  and  $\sigma^2 = 0.001$  for both GaBP and GEnBP. GEnBP has additional hyperparameters  $\eta^2 = 0.1$  and  $N = 64$ . We cap the number of iterations of message-propagation descent steps at 150. We relinearise or re-simulate after 10 message-propagation steps.

### A.1. System identification

In the system identification problem our goal is to estimate the time-invariant latent system parameter  $\mathbf{q}$ . This parameter influences all states in the Hidden Markov Model, where  $\mathbf{x}_0$  represents the unobserved initial state, and subsequent states  $\mathbf{x}_1, \mathbf{x}_2, \dots$  evolve over time. Each state  $\mathbf{x}_i$  is associated with an observed state  $\mathbf{y}_i$ , as depicted in Figure 4.

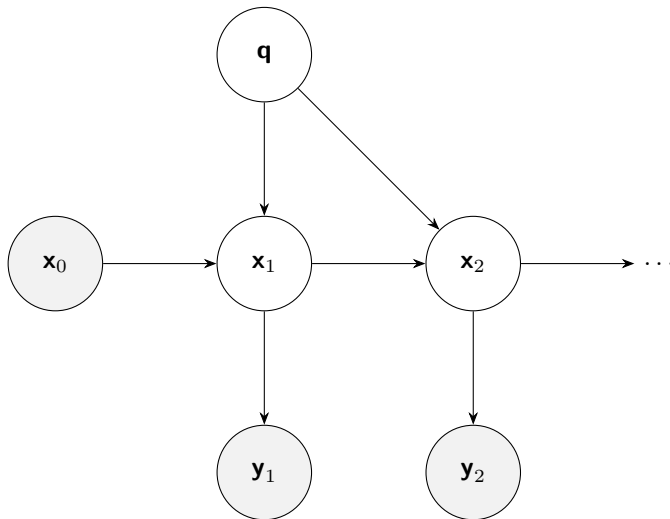


Figure 4: Generative model for the system identification problem, with latent system parameter  $\mathbf{q}$ , where all states depend on  $\mathbf{q}$  and the previous state. Observed states are shaded.

### A.2. 1D transport problem

States are one-dimensional vectors of length  $D_{\mathcal{Q}}$ .

$$\begin{aligned} \mathcal{P}_{\mathbf{x}}(\mathbf{x}_{t-1}, \mathbf{q}) &:= \text{shift}_k(g\mathbf{x}_{t-1} + (1-g)\mathbf{q} * \mathbf{b}) + \epsilon_{\text{process}} \\ \mathcal{P}_{\mathbf{y}}(\mathbf{x}_t) &:= \text{downsample}_{\ell}(\mathbf{x}_t) + \epsilon_{\text{obs}} \end{aligned}$$

$\mathcal{P}_{\mathbf{q}}$ , the prior for  $\mathbf{q}$ , draws periodic functions of the form  $F(\theta; \mu, \kappa, A) = A \cdot e^{\kappa \cos(\frac{k * 2\pi}{D_{\mathcal{Q}}} - \mu)}$  for  $k \in \{0, 1, D_{\mathcal{Q}} - 1\}$ , where  $\mu \sim \text{Uniform}[0, 2\pi]$ , is the phase,  $\kappa \sim \chi^2(\sqrt{2\pi})$ , and  $A = 9$ , i.e. the prior belief about amplitude is diffuse, but encodes smoothness and periodicity.  $\text{downsample}_{\ell}$  is a downsampling operator, which takes every  $\ell$ th element of the input vector.

The inference problem is to estimate the parameter  $\mathbf{q}$  given the sequence of observations  $\{\mathbf{y}_t\}$  and the initial state  $\mathbf{x}_0$ .

The number of timesteps is  $T = 10$ .

### A.3. Navier-Stokes system

The Navier-Stokes equation defines a classic problem in fluid modeling, whose solution is of interest in many engineering applications. A full introduction to the Navier-Stokes equation is beyond the scope of this paper; see Ferziger et al. (2019) or one of the many other introductions.

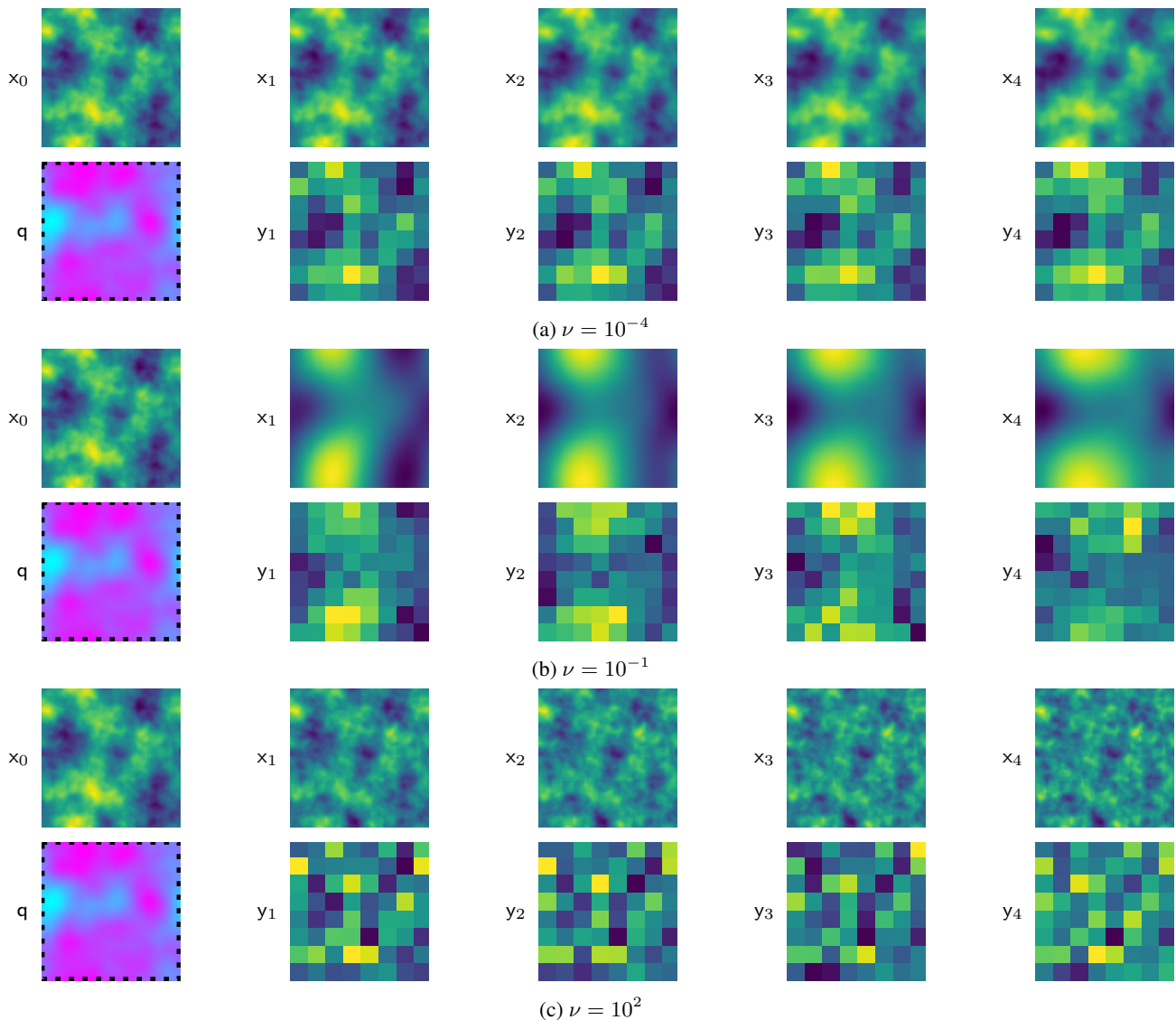


Figure 5: Three different Navier-Stokes simulations, with  $\Delta t = 0.2$  and varying value of viscosity  $\nu$ . The simulation is run on a  $64 \times 64$  grid; observations are  $8 \times 8$  and corrupted by white Gaussian noise with st  $\sigma = 0.1$  relative to a normalize unit scale for the simulations.

Our implementation here is a 2D incompressible flow, solved using a spectral method with pytorch implementation from a simulator Li et al. (2020). Defining vorticity  $\omega = \frac{\partial v}{\partial x} - \frac{\partial u}{\partial y}$  and streamfunction  $\psi$  which generates the velocity field by

$$u = \frac{\partial \psi}{\partial y}$$

$$v = -\frac{\partial \psi}{\partial x}$$

the Navier Stokes equations are

1. Poisson equation  $\nabla^2 \psi = -\omega$
2. Vorticity equation  $\frac{\partial \omega}{\partial t} + u \frac{\partial \omega}{\partial x} + v \frac{\partial \omega}{\partial y} = \nu \nabla^2 \omega$

The discretisation of the equation is onto an  $d \times d$  finite element basis for the domain, where each point summarises the vorticity field at that point. At each discretised time-step we inject additive mean-zero ( $d^2$ )-dimensional Gaussian white noise  $\boldsymbol{\nu}_t \sim \mathcal{N}(\mathbf{0}, \sigma_\eta^2 \mathbf{I})$  and static forcing term  $\mathbf{q}$  to the velocity term before solving the equation.

2d matrices are represented as 2d vectors by stacking and unstacking as needed, so  $\mathbf{x}_t = \text{vec}(\psi)$ .  $\mathbf{y} = \text{downsample}_\ell(\mathbf{x}_t) + \boldsymbol{\eta}$ , where  $\boldsymbol{\eta} \sim \mathcal{N}(\mathbf{0}, \sigma_\eta^2 \mathbf{I})$  is the observation noise.

Initial state and forcings are sampled from a discrete periodic Gaussian random field with

$$PSD(k) = \sigma^2 (4\pi^2 \|k\|^2 + \tau^2)^{-\alpha}. \tag{30}$$

## B. Experimental details and additional results

### B.1. Hardware configuration

Timings are conducted on Dell PowerEdge C6525 Server AMD EPYC 7543 32-Core Processors running at 2.8 GHz (3.7 GHz turbo) with 256 MB cache. Float precision is set to 64 bits for all calculations. Memory limit is capped to 32Gb. Execution time is capped to 119 minutes.

### B.2. Ensemble size

In the main text, we have left the matter of ensemble size  $N$  open. On one hand, ensembles of order  $N \approx 10^2$  seem to be ample for the problems we have considered. We might be concerned that the trade-off of increasing ensemble size is unclear; on one hand many computational costs scale relatively simply as  $\mathcal{O}(D^N 2 + N^3)$  (App I). On the other, we do not know how much extra precision we gain in general by increasing  $N$ . In Fig. 6 we show a small experiment to examine this trade-off, where the ensemble size is increased from  $N = 16$  to  $N = 512$  in steps of size 16. The problem shows a rapid improvement as the ensemble increases to  $N = 64$ , but diminishing marginal returns. There is no clear cut-off as such, but we specify  $N = 64$  as a default value for the experiments in the main text.

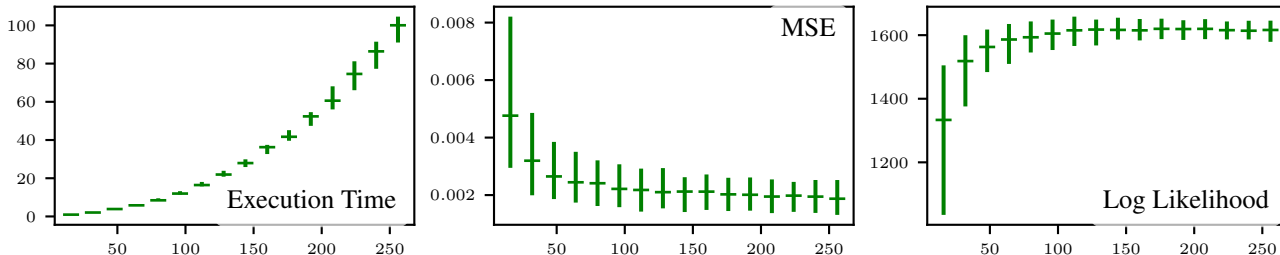


Figure 6: Performance of GENBP with varying ensemble size  $N$  for the 1d transport system identification problem (App A.2). Confidence intervals are empirical 95% intervals based on  $n = 80$  independent runs.

## C. Minimum viable introduction to probabilistic graphical models

The field of probabilistic graphical models is mature and vast. We refer the reader to Koller and Friedman (e.g. 2009); Wainwright and Jordan (e.g. 2008, and references therein) for a thorough introduction. A miniature introduction sufficient for this paper may be found here.

For the purposes of the current paper, it is sufficient to understand that this is the framework that we use to enable inference in complicated hierarchical systems with partial observations. Consider, for example, the hierarchical process in Fig. 7, which is a simplified representation of a weather model. An oceanic physics simulator and an atmospheric physics simulator provide forward predictions of the state of the ocean and atmosphere, and influence each other through physical coupling. Each of these dynamic systems is observed on a different time schedule by some form of telemetry (thermal satellite imagery for the oceans, phase radar for the atmosphere). All observations and state are high-dimensional, noisy and governed by nonlinear partial differential equations, including the observation models. Our primary target of inference is the 1-step ahead forward prediction for the atmosphere model. We could imagine many extensions of this, for example, to simultaneously learn the parameters of the observation or physics models as we learn their states.

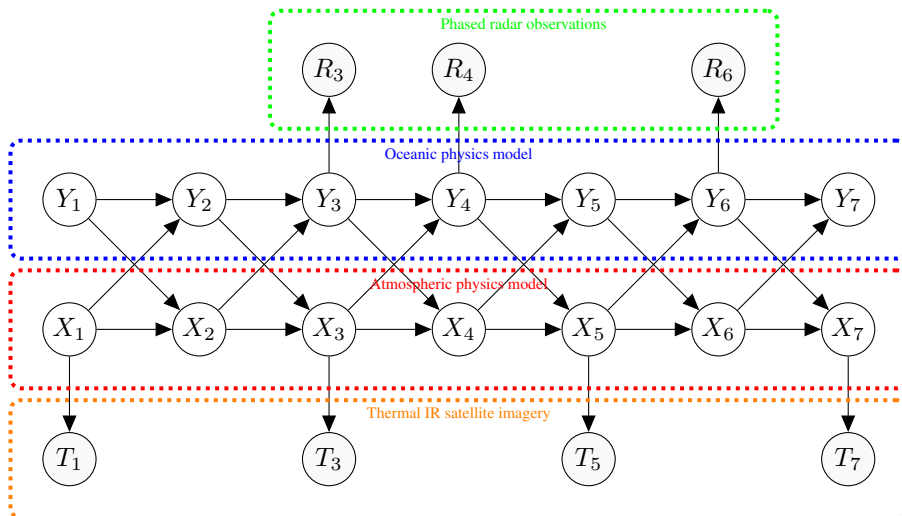


Figure 7: A complicated graphical model structure arising from a weather prediction problem. The model includes an oceanic physics simulator, an atmospheric physics simulator, phased radar observations, and thermal IR satellite imagery. The model is high-dimensional, noisy, and governed by nonlinear partial differential equations.

Graphical model formalisms provide a means of estimating states and parameters in these systems; the essential idea is that if we can find a set of rules that work for inference for arbitrary models, then we can apply them to complicated models like this. This paper introduces such a generic set of rules, which in-principle applies to arbitrarily complex graphical models, although scaling up to the complexity of the model in Fig. 7 is out of scope for a short methodological paper such as this.

### C.1. Directed graphs and factor graphs

We begin with the structural equations defining the model. By sampling from the distribution over these ancestral variables then iteratively applying the generative model (31), we obtain samples from the joint prior distribution of all random variates from the model. The state is jointly

$$\mathbf{x} = \begin{bmatrix} \mathbf{x}_{\mathcal{O}_1} \\ \vdots \\ \mathbf{x}_{\mathcal{O}_J} \end{bmatrix} = \begin{bmatrix} \mathcal{P}_1(\mathbf{x}_{\mathcal{I}_1}) \\ \vdots \\ \mathcal{P}_J(\mathbf{x}_{\mathcal{I}_J}) \end{bmatrix}. \quad (31)$$

The following conditions must hold for this to define a valid structural equation model

1.  $\forall j, \mathcal{O}_j \cap \mathcal{I}_j = \emptyset$  (no self-loop in a step).
2. If  $v \in \mathcal{O}_j$ , then for  $k > j$ ,  $v$  appears only in  $\mathcal{I}_k$ .

This defines a directed acyclic graph (DAG) over the variables, where the nodes are the variables and the edges are the generating equations. Each generating equation  $j$  induces an associated density  $p(\mathbf{x}_{\mathcal{O}_j} | \mathbf{x}_{\mathcal{I}_j})$ . The associated joint density is

$$p(\mathbf{x}) = \prod_j p(\mathbf{x}_{\mathcal{O}_j} | \mathbf{x}_{\mathcal{I}_j}). \quad (32)$$

Under some mild technical conditions (the local Markov condition, faithfulness and consistence - see Koller and Friedman (2009)), the representation given by the graph and the structural equations is equivalent to the joint distribution over the variables; We assume these conditions throughout.

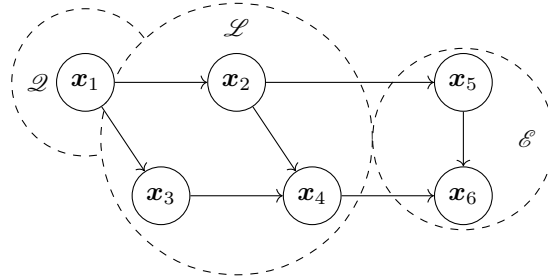
Hereafter we use the following specific generative model as a running example:

$$\begin{bmatrix} \mathbf{x}_1 \\ \mathbf{x}_2 \\ \mathbf{x}_3 \\ \mathbf{x}_4 \\ \mathbf{x}_5 \\ \mathbf{x}_6 \end{bmatrix} = \begin{bmatrix} \mathcal{P}_1() \\ \mathcal{P}_{12}(\mathbf{x}_1) \\ \mathcal{P}_{12}(\mathbf{x}_1) \\ \mathcal{P}_{234}(\mathbf{x}_2, \mathbf{x}_3) \\ \mathcal{P}_{25}(\mathbf{x}_2) \\ \mathcal{P}_{456}(\mathbf{x}_4, \mathbf{x}_5) \end{bmatrix}. \quad (33)$$

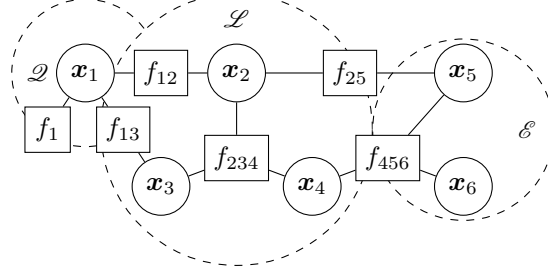
It is diagrammed in Fig 8 as a running example of the formalism. Its associated density can be factorised as

$$p(\mathbf{x}) = p_1(\mathbf{x}_1)p_{12}(\mathbf{x}_2|\mathbf{x}_1)p_{13}(\mathbf{x}_3|\mathbf{x}_1)p_{25}(\mathbf{x}_5|\mathbf{x}_2)p_{234}(\mathbf{x}_4|\mathbf{x}_2, \mathbf{x}_3)p_{456}(\mathbf{x}_6|\mathbf{x}_4, \mathbf{x}_5). \quad (34)$$

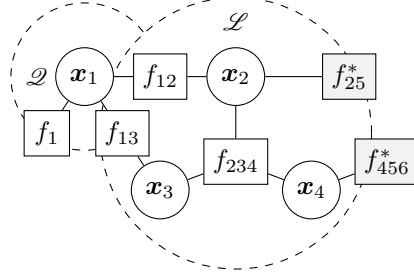
The directed generative model  $\mathcal{M}$ , and equivalently, conditional density, corresponds to 8a.



(a) Prior directed graph of generative model  $\mathcal{M}$ ,  $p(\mathbf{x}) = p_1(\mathbf{x}_1)p_{12}(\mathbf{x}_2|\mathbf{x}_1)p_{13}(\mathbf{x}_3|\mathbf{x}_1)p_{25}(\mathbf{x}_5|\mathbf{x}_2)p_{234}(\mathbf{x}_4|\mathbf{x}_2, \mathbf{x}_3)p_{456}(\mathbf{x}_6|\mathbf{x}_4, \mathbf{x}_5)$ .



(b) Prior factor graph  $\mathcal{G}$  for generative model  $\mathcal{M}$ ,  $p(\mathbf{x}) = f_1(\mathbf{x}_1)f_{12}(\mathbf{x}_1, \mathbf{x}_2)f_{13}(\mathbf{x}_1, \mathbf{x}_3)f_{234}(\mathbf{x}_2, \mathbf{x}_3, \mathbf{x}_4)f_{25}(\mathbf{x}_2, \mathbf{x}_5)f_{456}(\mathbf{x}_4, \mathbf{x}_5, \mathbf{x}_6)$ .



(c) Posterior factor graph  $\mathcal{G}^*$  of generative model  $\mathcal{M}$  after observing  $\mathbf{x}_5$  and  $\mathbf{x}_6$ ,  $p(\mathbf{x}_1, \mathbf{x}_2, \mathbf{x}_3, \mathbf{x}_4|\mathbf{x}_5, \mathbf{x}_6) \propto f_1(\mathbf{x}_1)f_{12}(\mathbf{x}_1, \mathbf{x}_2)f_{13}(\mathbf{x}_1, \mathbf{x}_3)f_{234}(\mathbf{x}_2, \mathbf{x}_3, \mathbf{x}_4)f_{25}^*(\mathbf{x}_2)f_{456}^*(\mathbf{x}_4)$

Figure 8: The graphical model variants used in this paper for example model (8): (a) prior generative graph, (b) prior factor graph, and (c) posterior factor graph; each with query nodes  $\mathcal{Q} = \{1\}$ , latent nodes  $\mathcal{L} = \{2, 3, 4\}$ , and observed nodes  $\mathcal{E} = \{5, 6\}$ .

The directed graphical model has the advantage of being intuitive, but it is not the most convenient for inference.

The factor graph form (Frey et al., 1997; Kschischang et al., 2001) discards the directions of the arrows induced by the generative models and works only with generic factors, transforming

$$p(\mathbf{x}_1|\mathbf{x}_2) \rightarrow f(\mathbf{x}_1, \mathbf{x}_2). \quad (35)$$

Our running example (34) becomes

$$p(\mathbf{x}) = f_1(\mathbf{x}_1)f_{12}(\mathbf{x}_1, \mathbf{x}_2)f_{13}(\mathbf{x}_1, \mathbf{x}_3)f_{234}(\mathbf{x}_2, \mathbf{x}_3, \mathbf{x}_4)f_{25}(\mathbf{x}_2, \mathbf{x}_5)f_{456}(\mathbf{x}_4, \mathbf{x}_5, \mathbf{x}_6). \quad (36)$$

The corresponding factor graph is shown in Fig. 8b. The factor graph is a bipartite graph with nodes corresponding to both variables and factor nodes. This representation has the advantage that simple approximate belief-updating message-passing rules may be written down for it. These rules we introduce in a sec. C.2.

We introduce one final graph transformation of use in this paper, which produces the conditional graph. We recall (3) that in practice we are interested in the evidence-conditional, posterior distribution,  $\mathbf{x}_{\mathcal{Q}}$  given the evidence variables  $\mathbf{x}_{\mathcal{E}} = \mathbf{x}_{\mathcal{E}}^*$ , i.e.

$$p(\mathbf{x}_{\mathcal{Q}}|\mathbf{x}_{\mathcal{E}}=\mathbf{x}_{\mathcal{E}}^*) = \frac{p(\mathbf{x}_{\mathcal{Q}}, \mathbf{x}_{\mathcal{E}}=\mathbf{x}_{\mathcal{E}}^*)}{p(\mathbf{x}_{\mathcal{E}}=\mathbf{x}_{\mathcal{E}}^*)} \quad (37)$$

$$= \frac{\int p(\mathbf{x}_{\mathcal{Q}}, \mathbf{x}_{\mathcal{L}}, \mathbf{x}_{\mathcal{E}}=\mathbf{x}_{\mathcal{E}}^*)d\mathbf{x}_{\mathcal{L}}}{\int p(\mathbf{x}_{\mathcal{Q}}, \mathbf{x}_{\mathcal{L}}, \mathbf{x}_{\mathcal{E}}=\mathbf{x}_{\mathcal{E}}^*)d\mathbf{x}_{\mathcal{Q}}d\mathbf{x}_{\mathcal{L}}}. \quad (38)$$

This can also be represented as a factor graph, as shown in Fig. 8c. The rule in this case is simply to use the factor graph corresponding to the factorisation induced by the posterior, which has a slightly different set of factors, since the observed nodes are no longer random, e.g.

$$p(\mathbf{x}_{\mathcal{Q}}|\mathbf{x}_{\mathcal{E}}=\mathbf{x}_{\mathcal{E}}^*) \propto p_1(\mathbf{x}_1)p_{12}(\mathbf{x}_2|\mathbf{x}_1)p_{13}(\mathbf{x}_3|\mathbf{x}_1)p_{234}(\mathbf{x}_4|\mathbf{x}_2, \mathbf{x}_3)p_{25}(\mathbf{x}_2|\mathbf{x}_5=\mathbf{x}_5^*)p_{456}(\mathbf{x}_4|\mathbf{x}_5=\mathbf{x}_5^*, \mathbf{x}_6=\mathbf{x}_6^*) \quad (39)$$

$$\propto f_1(\mathbf{x}_1)f_{12}(\mathbf{x}_1, \mathbf{x}_2)f_{13}(\mathbf{x}_1, \mathbf{x}_3)f_{234}(\mathbf{x}_2, \mathbf{x}_3, \mathbf{x}_4)f_{25}^*(\mathbf{x}_2)f_{456}^*(\mathbf{x}_4). \quad (40)$$

## C.2. Factor Graph Gaussian Belief Propagation

Basic loopy belief propagation (Murphy et al., 1999) is a simple and efficient algorithm for approximate inference of marginals over certain variables in factor graphs. There is a rich literature on when and how this algorithm converges to the true marginal, (Wainwright and Jordan, 2008; Yedidia et al., 2005). We do not concern ourselves with those details in this work, but simply follow industrial practice (e.g. Dellaert and Kaess, 2017) in treating it as a good enough approximation for our purposes. Following the terminology of Ortiz et al. (2021).

**Proposition 1** (Belief Propagation on Factor Graphs). *The following messages,*

$$m_{f_j \rightarrow \mathbf{x}_k} = \int \left( f_j(\mathbf{x}_{\mathcal{N}_j}) \prod_{i \in \mathcal{N}_j \setminus k} m_{\mathbf{x}_i \rightarrow f_j} \right) d\mathbf{x}_{\mathcal{N}_j \setminus k} \quad (5)$$

$$m_{\mathbf{x}_k \rightarrow f_j} = \prod_{s \in \mathcal{N}_k \setminus j} m_{f_s \rightarrow \mathbf{x}_k}, \quad (6)$$

*iteratively and synchronously propagated between all the nodes in the associated factor graph, yield the approximate marginal at target variable node,*

$$b_{\mathcal{G}}(\mathbf{x}_k) := \prod_{s \in \mathcal{N}_k} m_{f_s \rightarrow \mathbf{x}_k} \approx \int p(\mathbf{x})d\mathbf{x}_{\setminus k}. \quad (7)$$

*The fixed points of this iteration are the fixed points of the Bethe approximation to the target marginal.*

The factor graph belief propagation algorithm for generic factor graphs using these messages is presented Algorithm 3.

## C.3. Gaussian Factor updates

Finally we note that the factor graph formalism is particularly convenient for Gaussian models, as the Gaussian density is closed under multiplication, conditioning and marginalisation. We introduced this in sec 2.2.3, but write it out in full here.

As an exponential family distribution (Wainwright and Jordan, 2008), it become convenient to work with Gaussians in canonical form Eustice et al. (2006). We write  $\phi_M(\mathbf{x}; \mathbf{m}, \mathbf{K})$  for  $\phi_M$  the Gaussian density with moment parameters mean  $\mathbf{m}$  and covariance  $\mathbf{K}$ .

---

**Algorithm 3** Loopy Low-rank Belief Propagation over Factor Graph  $\mathcal{G}$ 


---

**Require:** Factor graph  $\mathcal{G}$  with variable nodes  $\{\mathbf{x}_k\}_k$  and factor nodes  $\{f_j\}_j$

**Require:** Initial messages  $\mathbf{x}_k \rightarrow f_j$  and  $f_j \rightarrow \mathbf{x}_k$

**Ensure:** Approximate marginal beliefs  $b(\mathbf{x}_k)$  for all  $\mathbf{x}_k \in \mathcal{G}$

```

1: Initialize message queues  $Q_{\mathbf{x}_k \rightarrow f_j}$  and  $Q_{f_j \rightarrow \mathbf{x}_k}$  to be empty
2: while not converged do
3:   for each factor  $f_j \in \mathcal{G}$  do
4:     for each variable  $\mathbf{x}_k \in \mathcal{N}_{f_j}$  do
5:       Send factor to variable message (5) to each neighbour
6:     end for
7:   end for
8:   for each variable  $\mathbf{x}_k \in \mathcal{G}$  do
9:     for each factor  $f_j \in \mathcal{N}_{\mathbf{x}_k}$  do
10:      Send variable to factor message (6) to each neighbour
11:    end for
12:    Update belief  $b(\mathbf{x}_k)$  (7)
13:  end for
14:  Check for convergence criteria
15: end while
16: Return  $b(\mathbf{x}_k)$  for all  $\mathbf{x}_k \in \mathcal{G}$ 

```

---

**Proposition 6.** As in Proposition 1, we partition the random vector  $\mathbf{x}_j \sim \phi_M \left( \begin{bmatrix} \mathbf{x}_k \\ \mathbf{x}_\ell \end{bmatrix}; \begin{bmatrix} \mathbf{m}_k \\ \mathbf{m}_\ell \end{bmatrix}, \begin{bmatrix} \mathbf{K}_{kk} & \mathbf{K}_{k\ell} \\ \mathbf{K}_{\ell k} & \mathbf{K}_{\ell\ell} \end{bmatrix} \right)$ . We define  $\hat{\mathbf{K}} := (\mathbf{K}_{jj}^{-1} + \mathbf{K}'_{jj}{}^{-1})^{-1}$ . Where the node and factors are Gaussian, the operations of Proposition 1 have the following form,

$$\text{Conditioning: } \phi_M(\mathbf{x}_j; \mathbf{m}_j, \mathbf{K}_{jj}), \mathbf{x}_k^* \mapsto \phi_M(\mathbf{x}_\ell; \mathbf{m}_\ell + \mathbf{K}_{\ell k} \mathbf{K}_{kk}^{-1}(\mathbf{x}_k^* - \mathbf{m}_k), \mathbf{K}_{\ell\ell} - \mathbf{K}_{\ell k} \mathbf{K}_{kk}^{-1} \mathbf{K}_{k\ell}); \quad (41)$$

$$\text{Marginalisation: } \phi_M(\mathbf{x}_j; \mathbf{m}_j, \mathbf{K}_{jj}) \mapsto \phi_M(\mathbf{x}_k; \mathbf{m}_k, \mathbf{K}_{kk}); \quad (42)$$

$$\text{Multiplication: } \phi'_M(\mathbf{x}_j; \mathbf{m}'_j, \mathbf{K}'_{jj}), \phi_M(\mathbf{x}_k; \mathbf{m}_k, \mathbf{K}_{kk}) \mapsto \phi_M(\mathbf{x}_j; \hat{\mathbf{K}}(\mathbf{K}_{jj}^{-1} \mathbf{m}_j + \mathbf{K}'_{kk}{}^{-1} \mathbf{m}'_j), \hat{\mathbf{K}}); \quad (43)$$

$$\phi'_C(\mathbf{x}_j; \mathbf{n}'_j, \mathbf{P}'_{jj}), \phi_C(\mathbf{x}_k; \mathbf{n}_k, \mathbf{P}_{kk}) \mapsto \phi_C(\mathbf{x}_j; \mathbf{n}'_j + \mathbf{n}_j, \mathbf{P}' + \mathbf{P}). \quad (44)$$

*Proof.* e.g. Bickson (2009). □

The classic GaBP algorithm includes many more details not captured in these minimal rules. Most importantly, since GaBP is frequently applied to factors that are not truly Gaussian, it needs a rule for finding a Gaussian distribution which approximates some factor potential.

#### C.4. Gaussian approximation of non-Gaussian factor potentials

Throughout this section we assume without loss of generality that all factor potentials are bivariate with  $\mathbf{x}_2 = \mathcal{P}(\mathbf{x}_1)$ . If this is not the case, we can stack and relabel the variates to make it bivariate.

The classic choice for approximating the factor potential generated by a nonlinear process is *propagation-of-errors* a.k.a. the  $\delta$ -method (Dorfman, 1938), whose application to this problem is introduced in the main body of the text at (15). The  $\delta$ -method relies upon the approximation

$$\mathbb{E}f(\mathbf{x}_1) \approx f(\mathbb{E}\mathbf{x}_1). \quad (45)$$

When we estimate, e.g. the joint covariance of the factor potential, we choose

$$f : [\mathbf{x}] \mapsto \begin{bmatrix} \mathbf{x} \\ \mathcal{P}(\mathbf{x}) \end{bmatrix} \begin{bmatrix} \mathbf{x} \\ \mathcal{P}(\mathbf{x}) \end{bmatrix}^\top - \mathbb{E} \begin{bmatrix} \mathbf{x} \\ \mathcal{P}(\mathbf{x}) \end{bmatrix} \mathbb{E} \begin{bmatrix} \mathbf{x} \\ \mathcal{P}(\mathbf{x}) \end{bmatrix}^\top \quad (46)$$

The difference

$$\mathcal{E}_{\text{Jensen}}(\mathbf{x}_1, f) := \mathbb{E}f(\mathbf{x}_1) - f(\mathbb{E}\mathbf{x}_1) \quad (47)$$

is called the *Jensen Gap* and is one source of error in the linearisation. The Jensen gap may sometimes be bounded, e.g. in terms of the coefficient of Hölder continuity of  $f$  and the moments of  $\mathbf{x}_1$  (Gao et al., 2020). In practice, this seems to be rarely done.

Further,  $\mathcal{P}$  and thus  $f$ , for problems of interest is still intractable in even this simplified calculation, and thus the  $\delta$ -method further approximates it using a surrogate given by first-order Taylor expansion about the mean,

$$\hat{f}(\mathbf{x}) \approx f(\mathbb{E}\mathbf{x}_1) + \nabla_{\mathbf{x}'} f(\mathbf{x}')|_{\mathbf{x}'=\mathbb{E}\mathbf{x}_1} (\mathbf{x} - \mathbb{E}\mathbf{x}_1) \quad (48)$$

The error for evaluating the expectation of some Taylor approximation  $\hat{f}$  of  $f$  is

$$\mathcal{E}_{\text{Taylor}}(\mathbf{x}_1, f, \hat{f}) := \mathbb{E}f(\mathbf{x}_1) - \mathbb{E}\hat{f}(\mathbf{x}_1). \quad (49)$$

The ultimate approximation of the covariance by the  $\delta$  method will include both the Jensen gap and the Taylor error, and additionally the inputs may not even be Gaussian. We can say little generally about the contribution of all such errors; there do not seem to be any results justifying its optimality in terms of e.g. a variational bound. In practice we may choose alternative methods based on practical effectiveness on the problem of interest.

While the  $\delta$ -method is simple and easy, it is not the only choice, and is empirically not necessarily favourable in either compute or accuracy, which deficiency we address in the sequel.

#### D. Minimum viable introduction to the Ensemble Kalman Filter

The field of Ensemble Kalman methods is mature and vast. We refer the reader to e.g. Evensen (2009) and references therein for a thorough introduction. A miniature introduction sufficient for this paper may be found here.

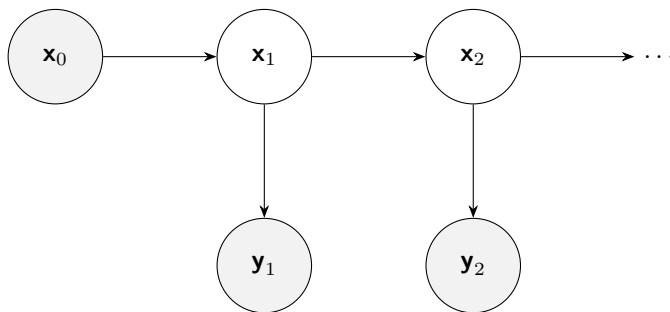


Figure 9: Generative model for state filtering problem, hidden states  $\mathbf{x}_t$  and observation  $\mathbf{y}_t$  for  $t = 1, 2, \dots$

The central idea is the following: given the state-space model (Fig. 9) with hidden states  $\mathbf{x}_t$  and observations  $\mathbf{y}_t$ , we wish to estimate the hidden states given the observations. The joint prior density of the state and observations is

$$p(\mathbf{x}_1, \mathbf{x}_2, \dots, \mathbf{x}_T, \mathbf{y}_1, \mathbf{y}_2, \dots, \mathbf{y}_T) =: p(\mathbf{x}_{0:T}, \mathbf{y}_{1:T}) \quad (50)$$

$$= \prod_{t=1}^T p(\mathbf{x}_t | \mathbf{x}_{t-1}) p(\mathbf{y}_t | \mathbf{x}_t). \quad (51)$$

Filtering leverages the fact that

$$p(\mathbf{x}_{0:T}, \mathbf{y}_{1:T}) = p(\mathbf{y}_T | \mathbf{x}_T) p(\mathbf{x}_T | \mathbf{x}_{T-1}) p(\mathbf{x}_{1:T-1}, \mathbf{y}_{1:T}) \quad (52)$$

so we can solve the problem by induction,

$$p(\mathbf{x}_{0:T} | \mathbf{y}_{1:T}) \propto p(\mathbf{y}_T | \mathbf{x}_T) p(\mathbf{x}_T | \mathbf{x}_{T-1}) p(\mathbf{x}_{1:T-1}, \mathbf{y}_{1:T-1}) \quad (53)$$

$$\propto p(\mathbf{y}_T | \mathbf{x}_T) p(\mathbf{x}_T | \mathbf{x}_{T-1}) p(\mathbf{x}_{T-1} | \mathbf{y}_{1:T-1}). \quad (54)$$

If we know  $p(\mathbf{x}_{1:T-1}|\mathbf{y}_{1:T-1})$ , to update to a new estimate of  $p(\mathbf{x}_T|\mathbf{y}_{1:T})$  we only need to be able to multiply its density by  $p(\mathbf{x}_T|\mathbf{x}_{T-1})p(\mathbf{y}_T|\mathbf{x}_T)$  and normalize; thus we can always calculate an estimate of the new state given the previous state estimate and the current observations.

Under Gaussianity of all distributions and linearity of all processes (e.g. Petersen and Pedersen (2012)) we can represent this density update in terms of the distribution parameters. For some  $\mathbf{m}_{T-1}, \mathbf{K}_{T-1}$ ,

$$p(\mathbf{x}_{T-1}|\mathbf{y}_{1:T-1}) = \phi_M(\mathbf{x}_{T-1}; \mathbf{m}_{T-1}, \mathbf{K}_{T-1}) \quad (55)$$

Linearity implies that there exist  $\mathbf{d}_{T-1}, \mathbf{F}_{T-1}, \mathbf{Q}_T$  the forward propagation operator  $\mathbf{x}_T = \mathcal{P}_{T-1}(\mathbf{x}_{T-1})$  of  $\mathbf{x}_T$  is

$$\mathbf{x}_T|\mathbf{x}_{T-1} = \mathcal{P}(\mathbf{x}_{T-1}) \quad (56)$$

$$= \mathbf{F}_{T-1}\mathbf{x}_{T-1} + \mathbf{d}_{T-1} + \boldsymbol{\epsilon}_T \quad (57)$$

where  $\boldsymbol{\epsilon} \sim \mathcal{N}(\mathbf{0}, \mathbf{Q}_T)$  so that

$$p\left(\begin{bmatrix} \mathbf{x}_{T-1} \\ \mathbf{x}_T \end{bmatrix} \middle| \mathbf{y}_{1:T-1}\right) = \phi_M\left(\begin{bmatrix} \mathbf{x}_{T-1} \\ \mathbf{x}_T \end{bmatrix}; \begin{bmatrix} \mathbf{m}_{T-1} \\ \mathbf{d}_{T-1} + \mathbf{F}_{T-1}\mathbf{m}_{T-1} \end{bmatrix}, \begin{bmatrix} \mathbf{K}_{T-1} & \mathbf{K}_{T-1}\mathbf{F}_{T-1}^\top \\ \mathbf{F}_{T-1}\mathbf{K}_{T-1} & \mathbf{F}_{T-1}\mathbf{K}_{T-1}\mathbf{F}_{T-1}^\top + \mathbf{Q}_T \end{bmatrix}\right). \quad (58)$$

The  $\mathbf{x}_T$  marginal is again Gaussian,

$$p(\mathbf{x}_T|\mathbf{x}_{T-1}, \mathbf{y}_{1:T-1}) = \phi_M(\mathbf{x}_T; \tilde{\mathbf{m}}_T, \tilde{\mathbf{K}}_T) \quad (59)$$

for  $\tilde{\mathbf{m}}_T = \mathbf{F}_{T-1}\mathbf{m}_{T-1} + \mathbf{d}_{T-1}$  and  $\tilde{\mathbf{K}}_T = \mathbf{F}_{T-1}\mathbf{K}_{T-1}\mathbf{F}_{T-1}^\top + \mathbf{Q}_T$ .

It remains to condition on the observation  $\mathbf{y}_T$ . We suppose that the measurement model  $\mathbf{y}_T = \mathcal{H}_T(\mathbf{x}_T)$  is linear and Gaussian, so that

$$\mathbf{y}_T|\mathbf{x}_T = \mathcal{H}(\mathbf{x}_T) \quad (60)$$

$$= \mathbf{H}_T\mathbf{x}_T + \mathbf{e}_T + \boldsymbol{\epsilon}_T \quad (61)$$

where  $\boldsymbol{\epsilon}_T \sim \mathcal{N}(\mathbf{0}, \mathbf{R}_T)$ . The joint density of  $\mathbf{x}_T$  and  $\mathbf{y}_T$  is

$$p\left(\begin{bmatrix} \mathbf{x}_T \\ \mathbf{y}_T \end{bmatrix} \middle| \mathbf{y}_{1:T-1}\right) = \phi_M\left(\begin{bmatrix} \mathbf{x}_T \\ \mathbf{y}_T \end{bmatrix}; \begin{bmatrix} \tilde{\mathbf{m}}_T \\ \mathbf{H}_T\tilde{\mathbf{m}}_T + \mathbf{e}_T \end{bmatrix}, \begin{bmatrix} \tilde{\mathbf{K}}_T & \tilde{\mathbf{K}}_T\mathbf{H}_T^\top \\ \mathbf{H}_T\tilde{\mathbf{K}}_T & \mathbf{H}_T\tilde{\mathbf{K}}_T\mathbf{H}_T^\top + \mathbf{R}_T \end{bmatrix}\right). \quad (62)$$

but we can use the standard formula for conditional Gaussian distributions to write

$$p(\mathbf{x}_T|\mathbf{y}_{1:T}) = \phi_M(\mathbf{x}_T; \mathbf{m}_T, \mathbf{K}_T) \quad (63)$$

where

$$\mathbf{K}_T = \tilde{\mathbf{K}}_T - \tilde{\mathbf{K}}_T\mathbf{H}_T(\mathbf{H}_T\tilde{\mathbf{K}}_T\mathbf{H}_T^\top + \mathbf{R}_T)^{-1}\mathbf{H}_T^\top\tilde{\mathbf{K}}_T^\top \quad (64)$$

$$\mathbf{m}_T = \tilde{\mathbf{m}}_T + \mathbf{K}_T\mathbf{H}_T^\top(\mathbf{H}_T\tilde{\mathbf{K}}_T\mathbf{H}_T^\top + \mathbf{R}_T)^{-1}(\mathbf{y}_T - \mathbf{H}_T\tilde{\mathbf{m}}_T - \mathbf{e}_T). \quad (65)$$

i.e. there is a closed-form update.

In practice, we may want to apply this method where at least one of the the state transition and observation models is nonlinear. The Extended Kalman Filter (EKF), uses a linearization of the state transition and observation models to approximate the update. We instead find a linear approximation to the state transition (57) and observation (61) models, by propagation of errors, setting

$$\mathbf{d}_{T-1} \approx \mathbb{E}[\mathcal{P}_{T-1}(\mathbf{m}_{T-1})] \quad (66)$$

$$\mathbf{F}_{T-1} \approx \nabla_{\mathbf{x}_{T-1}} \mathbb{E}[\mathcal{P}_{T-1}(\mathbf{m}_{T-1})] \quad (67)$$

$$\mathbf{e}_T \approx \mathbb{E}[\mathcal{H}_T(\tilde{\mathbf{m}}_T)] \quad (68)$$

$$\mathbf{H}_T \approx \nabla_{\mathbf{x}_T} \mathbb{E}[\mathcal{H}_T(\tilde{\mathbf{m}}_T)]. \quad (69)$$

and  $Q_T = \sigma^2 I$ ,  $R_T = \gamma^2 I$  are set to some diagonal covariance matrices. This type of linearised approximation is also used in the GaBP algorithm.

The EnKF takes a different approach to approximate inference, finding sample-based alternatives to the forward-propagation (59) and the observations update (63) Where the GaBP and EKF method summarises inference in terms of the parameters of a Gaussian distribution, the EnKF summarises the joint distribution in terms of an *ensemble* of Monte Carlo samples, i.e. a matrix of  $N$  samples,  $X := [\mathbf{x}^{(n)}]_{1 \leq n \leq N}$  drawn i.i.d. from the prior distribution,  $\mathbf{x}^{(n)} \sim \phi_M(\mathbf{x}; \mathbf{m}, K)$ . We reprise the definitions introduced in 2.3 by which the statistics of ensemble  $X$  define an implied Gaussian density,  $\mathbf{x} \sim \phi_M(\mathbf{x}; \bar{X}, \widehat{\text{Var}}_V X)$ .

$$\begin{aligned} A_N &:= \left[ \frac{1}{N} \quad \cdots \quad \frac{1}{N} \right]^\top, \\ B_N &:= [1 \quad \cdots \quad 1] \\ C_N &:= I_N - A_N B_N \\ \bar{X} &:= X A_N \end{aligned} \quad \begin{array}{l} \text{Ensemble mean} \\ \text{Ensemble deviation} \end{array} \quad (17)$$

$$\check{X} := X - X A_N B_N = X C_N. \quad \text{Ensemble deviation} \quad (18)$$

$$\widehat{\mathbb{E}} X = \bar{X} \quad (19)$$

$$\widehat{\text{Var}}_V X = \frac{1}{N-1} \check{X} \check{X}^\top + V \quad (20)$$

$$\widehat{\text{Cov}}(X, Y) = \frac{1}{N-1} \check{X} \check{Y}^\top \quad (21)$$

$V$  is a diagonal matrix *nugget* term, typically set to  $\sigma^2 I$ .

The EnKF equivalent of the Kalman filter forward joint distribution (58) is then

$$\begin{bmatrix} X_{T-1} \\ X_T \end{bmatrix} \Big| \mathbf{y}_{1:T-1} = \begin{bmatrix} X_{T-1} | \mathbf{y}_{1:T-1} \\ \mathcal{P}(X_{T-1} | \mathbf{y}_{1:T-1}) \end{bmatrix}. \quad (70)$$

By assumption this means that if we wished to calculate the density of the joint state, it would be

$$p(\mathbf{x}_{T-1}, \mathbf{x}_T | \mathbf{y}_{1:T-1}) = \phi_M \left( \begin{bmatrix} \mathbf{x}_{T-1} \\ \mathbf{x}_T \end{bmatrix}; \begin{bmatrix} \widehat{\mathbb{E}} X_T \\ \widehat{\mathbb{E}}[\mathcal{P}(X_T)] \end{bmatrix}, \begin{bmatrix} \widehat{\text{Var}}_V X_T & \widehat{\text{Cov}}(X_T, \mathcal{P}(X_T)) \\ \widehat{\text{Cov}}(\mathcal{P}(X_T), X_T) & \widehat{\text{Var}}_U \mathcal{P}(X_T) \end{bmatrix} \right). \quad (71)$$

The marginal (59) is simply the truncation of the above.

It turns out that we never need to explicitly evaluate such a density, because of the following result:

**Proposition 2.** Partition  $\mathbf{x} = \begin{bmatrix} \mathbf{x}_k \\ \mathbf{x}_\ell \end{bmatrix}$  so  $X = \begin{bmatrix} X_k \\ X_\ell \end{bmatrix}$ , and

$$X \sim \phi_M \left( \begin{bmatrix} \mathbf{x}_k \\ \mathbf{x}_\ell \end{bmatrix}; \begin{bmatrix} \bar{X}_k \\ \bar{X}_\ell \end{bmatrix}, \begin{bmatrix} \widehat{\text{Var}}_V X_k & \widehat{\text{Cov}}(X_\ell, X_k) \\ \widehat{\text{Cov}}(X_k, X_\ell) & \widehat{\text{Var}}_V(X_\ell) \end{bmatrix} \right). \quad (22)$$

In ensemble form, conditioning (9) becomes

$$X, \mathbf{x}_k^* \mapsto X_\ell + \widehat{\text{Cov}}(X_\ell, X_k) \widehat{\text{Var}}_V^{-1}(X_k) (\mathbf{x}_k^* B - X_k) \quad (23)$$

The time cost of (23) is  $\mathcal{O}(N^3 + N^2 D_{\mathbf{x}_k})$ . Marginalisation (10) is simply truncation,  $X \mapsto X_k$ .

*Proof.* The equality (23) follows from 7 with the substitution of (22).

Notably we do not need to construct  $\widehat{\text{Var}}_V(X_\ell)$ , and can use Woodbury formula to efficiently solve the linear system involving  $\widehat{\text{Var}}_V^{-1}(X_k)$ .  $\square$

We can use this to calculate an observation-conditional update, since

$$\begin{bmatrix} X_T \\ Y_T \end{bmatrix} \Big| \mathbf{y}_{1:T-1} = \begin{bmatrix} X_T | \mathbf{y}_{1:T-1} \\ \mathcal{H}(X_T | \mathbf{y}_{1:T-1}) \end{bmatrix}. \quad (72)$$

We can use (23) to calculate  $X_T | \mathbf{y}_{1:T}$  by using  $\mathbf{y}_T$  as the observations  $\mathbf{x}_k^*$  in the update. We have thus obtained sampled from the filtered distribution without ever evaluating its density.

### D.1. Gaussian approximation of non-Gaussian factor potentials

As with the the GaBP, the EnKF is frequently applied to non-Gaussian distributions. Unlike the GaBP, we never use the  $\delta$ -method as in (15). Instead, the *empirical* joint (72) already finds the moments of an approximating distribution. The price we pay that as a stochastic approximation, we have now introduced aleatoric noise to the estimate. Despite this, the EnKF approximation is often more accurate than the GaBP, a fact intensely studied in the literature Furrer and Bengtsson (2007, e.g.), although once again few actionable analytic results are available (Le Gland et al., 2009; Kelly et al., 2014). Empirically, EnKF is nonetheless frequently SOTA.

Heuristically, we argue that this is because the EnKF samples from the full joint distribution. This avoids accruing error via the Jensen gap (46) or the Taylor expansion approximation (48) used in the GaBP, which samples only the mean. Explicitly, the propagation of errors in GaBP produces approximations like the following

$$\widehat{\text{Var}}^{\text{GaBP}} \begin{bmatrix} \mathbf{x}_1 \\ \mathbf{x}_2 \end{bmatrix} \simeq \begin{bmatrix} \text{Var} \mathbf{x}_1 & J(\mathbf{m}_1) \text{Var} \mathbf{x}_1 \\ \text{Var} \mathbf{x}_1 J(\mathbf{m}_1)^\top & J(\mathbf{m}_1) \text{Var} \mathbf{x}_1 J^\top(\mathbf{m}_1) \end{bmatrix} \quad (73)$$

where  $J(x)$  is the jacobian matrix of  $\mathcal{P}$  at  $x$ . In the EnKF, the joint variance is modeled by empirical samples,

$$\widehat{\text{Var}}^{\text{EnKF}} \begin{bmatrix} \mathbf{x}_1 \\ \mathbf{x}_2 \end{bmatrix} \simeq \widehat{\text{Var}}_{\sigma^2 \mathbf{I}} \begin{bmatrix} x^{(1)} & \dots & x^{(N)} \\ \mathcal{P}(x^{(1)}) & \dots & \mathcal{P}(x^{(N)}) \end{bmatrix} \quad (74)$$

$$= \sigma^2 \mathbf{I} + \begin{bmatrix} x^{(1)} & \dots & x^{(N)} \\ \mathcal{P}(x^{(1)}) & \dots & \mathcal{P}(x^{(N)}) \end{bmatrix} \begin{bmatrix} x^{(1)} & \dots & x^{(N)} \\ \mathcal{P}(x^{(1)}) & \dots & \mathcal{P}(x^{(N)}) \end{bmatrix}^\top. \quad (75)$$

The relative quality of each of these updates is nontrivial to discover. Noting, however, that the EnKF estimates are frequently better in practice, and, as demonstrated at length in this paper, can be made computationally more efficient in high dimensions, we find out motivation for exploring the generalisation of the EnKF that drives the GEnBP algorithm.

### E. Matheron updates for Gaussian variates

The pathwise Gaussian process update (*Matheron update*), credited to Matheron by Wilson et al. (2021); Doucet (2010) is a method of simulating from a conditional of some jointly Gaussian variate. If

$$\begin{bmatrix} \mathbf{y} \\ \mathbf{w} \end{bmatrix} \sim \mathcal{N} \left( \begin{bmatrix} m_{\mathbf{y}} \\ m_{\mathbf{w}} \end{bmatrix}, \begin{bmatrix} \mathbf{K}_{\mathbf{y}\mathbf{y}} & \mathbf{K}_{\mathbf{y}\mathbf{w}} \\ \mathbf{K}_{\mathbf{w}\mathbf{y}} & \mathbf{K}_{\mathbf{w}\mathbf{w}} \end{bmatrix} \right) \quad (76)$$

then the moment of the  $\mathbf{w}$ -conditional distribution are

$$\mathbb{E}[\mathbf{y} \mid \mathbf{w}=\mathbf{w}^*] = m_{\mathbf{y}} + \mathbf{K}_{\mathbf{w}\mathbf{y}} \mathbf{K}_{\mathbf{w}\mathbf{w}}^{-1} (\mathbf{w}^* - m_{\mathbf{w}}) \quad \text{first moment} \quad (77)$$

$$\text{Var}[\mathbf{y} \mid \mathbf{w}=\mathbf{w}^*] = \mathbf{K}_{\mathbf{y}\mathbf{y}} - \mathbf{K}_{\mathbf{w}\mathbf{y}} \mathbf{K}_{\mathbf{w}\mathbf{w}}^{-1} \mathbf{K}_{\mathbf{y}\mathbf{w}}. \quad \text{second moment} \quad (78)$$

**Proposition 7.** For  $\begin{bmatrix} \mathbf{y} \\ \mathbf{w} \end{bmatrix}$  as in (76), the variates in the following mapping

$$\mathbf{y}, \mathbf{w}, \mathbf{w}^* \mapsto \mathbf{y} + \mathbf{K}_{\mathbf{w}\mathbf{y}} \mathbf{K}_{\mathbf{w}\mathbf{w}}^{-1} (\mathbf{w}^* - \mathbf{w}) \quad (79)$$

satisfy the moment conditions (77) and (78) and thus  $(\mathbf{y} + \mathbf{K}_{\mathbf{w}\mathbf{y}} \mathbf{K}_{\mathbf{w}\mathbf{w}}^{-1} (\mathbf{w}^* - \mathbf{w})) \stackrel{d}{=} (\mathbf{y} \mid \mathbf{w}=\mathbf{w}^*)$ .

*Proof.* Taking moments of (79)

$$\begin{aligned} \mathbb{E}[\mathbf{y} + \mathbf{K}_{\mathbf{w}\mathbf{y}} \mathbf{K}_{\mathbf{w}\mathbf{w}}^{-1} (\mathbf{w}^* - \mathbf{w})] &= m_{\mathbf{y}} + \mathbf{K}_{\mathbf{w}\mathbf{y}} \mathbf{K}_{\mathbf{w}\mathbf{w}}^{-1} (\mathbf{w}^* - m_{\mathbf{w}}) \\ \text{Var}[\mathbf{y} + \mathbf{K}_{\mathbf{w}\mathbf{y}} \mathbf{K}_{\mathbf{w}\mathbf{w}}^{-1} (\mathbf{w}^* - \mathbf{w})] &= \text{Var}[\mathbf{y}] + \text{Var}[\mathbf{K}_{\mathbf{w}\mathbf{y}} \mathbf{K}_{\mathbf{w}\mathbf{w}}^{-1} (\mathbf{w}^* - \mathbf{w})] + \text{Cov}(\mathbf{y}, \mathbf{K}_{\mathbf{w}\mathbf{y}} \mathbf{K}_{\mathbf{w}\mathbf{w}}^{-1} (\mathbf{w}^* - \mathbf{w})) + \text{Cov}(\mathbf{y}, \mathbf{K}_{\mathbf{w}\mathbf{y}} \mathbf{K}_{\mathbf{w}\mathbf{w}}^{-1} (\mathbf{w}^* - \mathbf{w}))^\top \\ &= \mathbf{K}_{\mathbf{y}\mathbf{y}} + \mathbf{K}_{\mathbf{w}\mathbf{y}} \mathbf{K}_{\mathbf{w}\mathbf{w}}^{-1} \mathbf{K}_{\mathbf{w}\mathbf{w}} \mathbf{K}_{\mathbf{w}\mathbf{w}}^{-1} \mathbf{K}_{\mathbf{y}\mathbf{w}} - 2 \mathbf{K}_{\mathbf{y}\mathbf{w}} \mathbf{K}_{\mathbf{w}\mathbf{w}}^{-1} \mathbf{K}_{\mathbf{w}\mathbf{y}} \\ &= \mathbf{K}_{\mathbf{y}\mathbf{y}} - \mathbf{K}_{\mathbf{w}\mathbf{y}} \mathbf{K}_{\mathbf{w}\mathbf{w}}^{-1} \mathbf{K}_{\mathbf{y}\mathbf{w}} \end{aligned}$$

we see that both first and second moment conditions are satisfied.  $\square$

Note that this update does not require us to calculate  $\mathbf{K}_{\mathbf{y}\mathbf{y}}$  and further, may be conducted without needing to evaluate the density of the observation.

## F. Nearly-low-rank matrices

Suppose the  $K = V + kLL^\top$  where  $L$  is a  $D \times N$  matrix,  $V$  is  $D \times D$  and  $V = \text{diag}(v)$  and  $k \in \{-1, 1\}$  is the *sign* of the matrix. We are primarily interested in such matrices in the case that  $N \ll D$ , which case we have called *nearly-low-rank*, when their computational properties are favourable for our purposes. This is in contrast to matrices with no particular exploitable structure, which we refer to as *dense*.

Throughout this section we assume that the matrices in question are positive definite; and that all operations are between conformable operations. We refer to the matrix  $L$  as the *component* of the nearly-low-rank matrix, and the diagonal matrix  $V$ .

If  $N \geq D$  the name is misleading since they are not truly *low-rank*; the identities we write here still hold, but are not computationally expedient.

### F.1. Multiplication by a dense matrix

The matrix product of an arbitrary matrix with a nearly-low-rank matrix may be calculated efficiently by grouping operations, since  $KX = VX \pm U(U^\top X)$ , which has a time cost of  $\mathcal{O}(ND^2)$  and which may be calculated without forming the full matrix  $K$ . The result is not in general also a nearly-low-rank matrix.

### F.2. Addition

The matrix sum of two nearly-low-rank matrices with the same sign is also a nearly-low-rank matrix. Suppose  $K = V + kLL^\top, K' = V' + kL'L'^\top$ ,

$$K + K' = V + V' + kLL^\top + kL'L'^\top \quad (80)$$

$$= V + V' + k \begin{bmatrix} L & L' \end{bmatrix} \begin{bmatrix} L & L' \end{bmatrix}^\top. \quad (81)$$

The new matrix, is also nearly low rank with has nugget term  $V + V'$  and component  $\begin{bmatrix} L & L' \end{bmatrix}$ .

### F.3. Cheap nearly-low-rank inverses

Inverses of nearly-low-rank matrices are once again nearly-low-rank matrices, and may be found efficiently.

**Proposition 8.** Choose nearly-low rank  $K = V + LL^\top$ , i.e. with sign  $k$  positive. Then its inverse

$$K^{-1} = V^{-1} - RR^\top \quad (82)$$

is also nearly-low-rank, of the same component dimension, but with a negative sign, with

$$R = V^{-1}L \text{ chol} \left( (I + L^\top V^{-1}L)^{-1} \right). \quad (83)$$

where  $\text{chol}(A)$  denotes a decomposition  $\text{chol}(A)\text{chol}(A)^\top = A$ .

*Proof.* Using the Woodbury identity,

$$\begin{aligned} K^{-1} &= V^{-1} - V^{-1}L(I + L^\top V^{-1}L)^{-1}L^\top V^{-1} \\ &= V^{-1} - RR^\top. \end{aligned}$$

□

**Proposition 9.** Choose nearly-low rank  $P = U - RR^\top$ , i.e. with sign  $k$  negative. Then its inverse

$$P^{-1} = U^{-1} - LL^\top \quad (84)$$

is also nearly-low-rank, of the same component dimension, but with a positive sign, with

$$L = U^{-1}R \text{ chol} \left( (-I + R^\top U^{-1}R)^{-1} \right). \quad (85)$$

*Proof.* Using the Woodbury identity,

$$P^{-1} = U^{-1} - U^{-1}R(-I + R^{\top}U^{-1}R)^{-1}R^{\top}U^{-1} \quad (86)$$

$$= U^{-1} + LL^{\top} \quad (87)$$

□

The cost of the inversion is the same for both,  $\mathcal{O}(N^2D + N^3) = \mathcal{O}(N^3)$  for the construction of the Cholesky factor, and  $\mathcal{O}(DN^2)$  for the requisite matrix multiplies. The space cost is  $\mathcal{O}(ND)$ .

For a given  $K = V + kLL^{\top}$ , the term  $(kI + L^{\top}V^{-1}L)$  is referred to as the *capacitance* of the matrix by convention.

#### F.4. Exact inversion when the component is high-rank

Suppose  $P = U - RR^{\top}$  where the  $D \times N$  components high rank, in the sense that  $N > D$ . Then the low rank inversion to calculate  $P^{-1}$  is no longer cheap, since the  $\mathcal{O}(N^D)$  cost is greater than naive inversion of the dense matrix, at  $\mathcal{O}(D^3)$ . In this case, it is cheaper to recover a nearly-low-rank inverse by an alternate method. Note that  $(U - P)^{-1} = U^{-1} - U^{-1}(U^{-1} - P^{-1})^{-1}U^{-1}$ . We find the eigendecomposition

$$P^{-1} = U^{-1} + LL^{\top} \quad (88)$$

for some  $L$ . Such an  $L$  is given by  $L = Q\Lambda^{1/2}$  for  $Q\Lambda Q^{\top} = P^{-1} - U^{-1}$  a spectral decomposition. In the case that the diagonal  $U$  is constant this may be found more efficiently.

If, instead, we wish to invert  $K = V + LL^{\top}$  we need to find  $(-V + K)^{-1} = -V^{-1} - V^{-1}(K^{-1} - V^{-1})^{-1}V^{-1}$ , so we decompose instead  $Q\Lambda Q = V^{-1}(K^{-1} - V^{-1})^{-1}V^{-1}$  and define  $R = Q\Lambda^{-1/2}$ . Then the nearly-low-rank form of the inverse is  $-V^{-1} - RR^{\top}$ .

#### F.5. Reducing component rank

We use the SVD to efficiently reduce the rank of the components in the nearly-low-rank matrix in the sense of finding a Frobenius-distance-minimising approximation.

Suppose  $K = V + LL^{\top}$  where  $L$  is a  $D \times M$  matrix,  $I$  is  $D \times D$  and  $V = \text{diag}(v)$ . Let  $YSZ^{\top}$  be the “thin” SVD of  $L$ , i.e.  $Y \in \mathbb{R}^{D \times M}$ ,  $S \in \mathbb{R}^{M \times M}$ ,  $Z \in \mathbb{R}^{M \times M}$  with  $Y^{\top}Y = I_N$ ,  $Z^{\top}Z = I_N$ , and  $S$  diagonal with non-negative entries. Then

$$LL^{\top} = YSZ^{\top}ZSY^{\top} = YS^2Y^{\top}.$$

First we note that should any singular values in  $S$  be zero, we may remove the corresponding columns of  $Y$  and  $Z$  without changing the product, so their exclusion is exact. Next, we note that if we choose the largest  $S$  singular values of  $S$ , setting the rest to zero, we obtain a Frobenius approximation of  $LL^{\top}$  of rank  $S$ .

An SVD that captures the top  $N$  singular values may be found by conventional thin SVD at a cost of  $\mathcal{O}(DN^2)$ .

## G. Gaussians with nearly-low-rank parameters

We recall the forms of the Gaussian density introduced in section 2.2.3, in *moments* form using the mean  $\mathbf{m}$  and covariance matrix  $K$ ,

$$\mathbf{x} \sim \mathcal{N}(\mathbf{m}, K) = \mathcal{N}(\mathbb{E}[\mathbf{x}], \text{Var}(\mathbf{x})).$$

and the *canonical* form,

$$\mathbf{x} \sim \mathcal{N}_C(\mathbf{n}, P) = \mathcal{N}_C(\text{Var}^{-1}(\mathbf{x})\mathbb{E}[\mathbf{x}], \text{Var}^{-1}(\mathbf{x})).$$

which uses the information vector  $\mathbf{n}$  and the *precision matrix*,  $P$  with  $\mathbf{n} = K^{-1}\mathbf{m}$ ,  $P = K^{-1}$ . The (equivalent) densities induced by these parameterisations are

$$f(\mathbf{x}) \propto \frac{1}{2}(\mathbf{x} - \mathbf{m})^{\top}K^{-1}(\mathbf{x} - \mathbf{m}) = \frac{1}{2}\mathbf{x}^{\top}P\mathbf{x} - \mathbf{n}^{\top}\mathbf{x}$$

We associate a given Gaussian ensemble with a moments-form Gaussian in the natural way,

$$X_{\sigma^2} \sim \mathcal{N}(\mathbf{m}, \mathbf{K}) = \mathcal{N}(\widehat{\mathbb{E}}[X], \widehat{\text{Var}}_{\sigma^2}(X))$$

introducing a parameter  $\sigma^2$  which we use to ensure invertibility of the covariance if needed.

We associate with each moments-form Gaussian a *canonical form* which may be cheaply calculated by using the by using the low-rank representation of the covariance prop 8,

$$\begin{aligned} X_{\sigma^2} &\sim \mathcal{N}(\mathbf{m}, \mathbf{K}) \\ \mathbf{m} &= \widehat{\mathbb{E}}(X) = \bar{X} \\ \mathbf{K} &= \widehat{\text{Var}}_{\sigma^2}(X) = \sigma^2 \mathbf{I} + \check{X}\check{X}^\top \\ &\Leftrightarrow \\ X_{\sigma^2} &\sim \mathcal{N}_C(\mathbf{n}, \mathbf{P}) \\ \mathbf{n} &= \widehat{\text{Var}}_{\sigma^2}^{-1}(X) \widehat{\mathbb{E}}(X) = \mathbf{P}\bar{X} \\ \mathbf{P} &= \widehat{\text{Var}}_{\sigma^2}^{-1}(X) = \sigma^{-2}\mathbf{I} - \mathbf{R}\mathbf{R}^\top. \end{aligned}$$

where we introduced  $\mathbf{R} = \check{X} \text{chol} \left( \left( \mathbf{I} + \sigma^{-2} \check{X}^\top \check{X} \right)^{-1} \right)$ .

We may recover  $\mathbf{m}$  and  $\mathbf{K}$  from  $\mathbf{n}$  and  $\mathbf{P}$  by

$$\begin{aligned} \mathbf{K} &= \mathbf{P}^{-1} \\ \mathbf{m} &= \mathbf{P}^{-1}\mathbf{n}. \end{aligned}$$

this time using the alternative low rank inverse formula 9.

## H. Ensemble recovery

Suppose that after belief propagation we update our belief about a given query variable node to  $b(\mathbf{x}_{\mathcal{Q}}) \sim \mathcal{N}_M(\mathbf{x}_{\mathcal{Q}}; \mathbf{m}, \mathbf{K}_{\mathcal{Q}})$ . In the Ensemble message passing setting we have nearly-low-rank  $\mathbf{K}_{\mathcal{Q}} = \mathbf{V}_{\mathcal{Q}} + \mathbf{L}_{\mathcal{Q}}\mathbf{L}_{\mathcal{Q}}^\top$ . In order to convert this belief into ensemble samples, we choose the transformation  $T$  which maps prior ensemble  $X_{\mathcal{Q}}$  from the previous iterate to an updated ensemble  $X'_{\mathcal{Q}} = T(X_{\mathcal{Q}})$  such that the (empirical) ensemble distribution is as similar as possible, in some metric  $d$  to  $\mathcal{N}_M(\mathbf{x}_{\mathcal{Q}}; \mathbf{m}, \mathbf{K}_{\mathcal{Q}})$ . Hereafter we suppress the subscript  $Q$  for compactness, and because what follows is generic for ensemble moment matching. This amounts to choosing

$$T = \operatorname{argmin}_{T^*} d(\mathcal{N}_M(\cdot; \widehat{\mathbb{E}}T(X), \widehat{\text{Var}}_{\sigma^2}T(X)), \mathcal{N}_M(\cdot; \mathbf{m}, \mathbf{K})), \quad (89)$$

We wish to do this *without forming*  $\mathbf{K} \in \mathbb{R}^{D \times D}$ , which may be prohibitively memory expensive, by exploiting its nearly-low-rank decomposition. We restrict ourselves to the family of affine transformations  $T_{\boldsymbol{\mu}, \mathbf{T}} : X \mapsto \boldsymbol{\mu} + \check{X}\mathbf{T}$  where the parameters  $\boldsymbol{\mu} \in \mathbb{R}^D$ ,  $\mathbf{T} \in \mathbb{R}^{N \times N}$  must be chosen. If we minimise between the belief and ensemble distributions empirical covariances, the solution is

$$\boldsymbol{\mu} = \widehat{\mathbb{E}}X \quad (90)$$

$$\mathbf{T} = \operatorname{argmin}_{\mathbf{T}} \left\| \widehat{\text{Var}}_{\sigma^2}(\check{X}\mathbf{T}) - \mathbf{K} \right\|_F^2 \quad (91)$$

$$= \operatorname{argmin}_{\mathbf{T}} \left\| \widehat{\text{Var}}_{\sigma^2}(T(X)) - \mathbf{L}\mathbf{L}^\top - \mathbf{V} \right\|_F^2 \quad (92)$$

$$= \operatorname{argmin}_{\mathbf{T}} \left\| \frac{\check{X}\mathbf{T}\mathbf{T}^\top\check{X}^\top}{N-1} - \mathbf{V}_{-\sigma^2} - \mathbf{L}\mathbf{L}^\top \right\|_F^2, \quad (93)$$

Here we have introduced  $\mathbf{V}_{-\sigma^2} := \mathbf{V} - \sigma^2\mathbf{I}$ . Note that minimisers of  $L$  with respect to  $\mathbf{T}$  are not unique, because  $L$  depends only on  $\mathbf{T}\mathbf{T}^\top$ . For example, we may take any orthogonal transformation  $\mathbf{U}$  of  $\mathbf{T}$  and obtain the same  $(\mathbf{T}\mathbf{U})(\mathbf{T}\mathbf{U})^\top =$

$\mathbb{T}\mathbb{U}\mathbb{U}^\top\mathbb{T}^\top = \mathbb{T}\mathbb{T}^\top$ . We instead optimise  $\mathbb{M} = \mathbb{T}\mathbb{T}^\top$  over the space of  $N \times N$  PSD matrices  $\mathbb{M}_+^N = \{\mathbb{M} \in \mathbb{R}^{N \times N} \mid \mathbb{M} = \mathbb{M}^\top, \mathbb{M} \succeq 0\}$ . That is, we consider the problem

$$\mathbb{M}^* = \operatorname{argmin}_{\mathbb{M} \in \mathbb{M}_+^N} L(\mathbb{M}) \quad (94)$$

where

$$L(\mathbb{M}) := \operatorname{argmin}_{\mathbb{M}} \left\| \frac{1}{N-1} \check{\mathbb{X}}\mathbb{M}\check{\mathbb{X}}^\top - \mathbb{L}\mathbb{L}^\top - \mathbb{V}_{-\sigma^2} \right\|_F^2. \quad (95)$$

This is a convex problem in  $\mathbb{M}$ . The derivatives are given by (Laue et al., 2018; 2020)

$$\begin{aligned} \nabla_{\mathbb{M}} L &= \frac{2}{N-1} \check{\mathbb{X}}^\top \left( \frac{\check{\mathbb{X}}\mathbb{M}\check{\mathbb{X}}^\top}{N-1} - \mathbb{L}\mathbb{L}^\top - \mathbb{V}_{-\sigma^2} \right) \check{\mathbb{X}} \\ &= \frac{2}{N-1} \left( \frac{\check{\mathbb{X}}^\top \check{\mathbb{X}}\mathbb{M}\check{\mathbb{X}}^\top \check{\mathbb{X}}}{N-1} - (\check{\mathbb{X}}^\top \mathbb{L})(\check{\mathbb{X}}^\top \mathbb{L})^\top - \check{\mathbb{X}}^\top \mathbb{V}_{-\sigma^2} \check{\mathbb{X}} \right) \end{aligned}$$

An unconstrained solution in  $\mathbb{M}'$  may be found by setting the gradient to zero,

$$\check{\mathbb{X}}^\top \check{\mathbb{X}}\mathbb{M}'\check{\mathbb{X}}^\top \check{\mathbb{X}} = (N-1) \left( \check{\mathbb{X}}^\top \mathbb{L}(\check{\mathbb{X}}^\top \mathbb{L})^\top + \check{\mathbb{X}}^\top \mathbb{V}_{-\sigma^2} \check{\mathbb{X}} \right).$$

This linear system may be solved at  $\mathcal{O}(N^3)$  cost for the ensemble size  $N$ . As  $\check{\mathbb{X}}^\top \check{\mathbb{X}}$  is Hermitian we also economise by using specialised methods such as pivoted LDL decomposition. Using the same decomposition we also find the required  $\mathbb{M}^* = \mathbb{T}\mathbb{T}^\top$ , choosing  $\mathbb{T} = \mathbb{U}(S^+)^{1/2}$ . By careful ordering of operations we may calculate the RHS with cost  $\mathcal{O}(DM^2)$  for a total cost of  $\mathcal{O}(N^3 + DN^2 + DM^2)$ .

## I. Computational costs

We summarise results from Ortiz et al. (2021) and sections 3.2 and 3.4 in Table 2. Note that GEnBP is never worse than linear in  $D$ , unlike GaBP. On the other hand, GaBP does not depend upon node degree  $K$  or ensemble size  $N$ .

Table 2: Computational Costs for Gaussian Belief Propagation and Ensemble Belief propagation for node dimension  $D$ , node degree  $K$ , ensemble size  $N$ . For simplicity, all variables are assumed to have the same dimension.

Operation		GaBP	GEnBP
Time Complexity	Simulation	$\mathcal{O}(1)$	$\mathcal{O}(N)$
	Error propagation	$\mathcal{O}(D^3)$	—
	Jacobian calculation	$\mathcal{O}(D)$	—
	Covariance matrix	$\mathcal{O}(D^2)$	$\mathcal{O}(N+D)$
	Factor-to-node message	$\mathcal{O}(D^3)$	$\mathcal{O}(K^3N^3 + DN^2K^2)$
	Node-to-factor message	$\mathcal{O}(D^2)$	$\mathcal{O}(1)$
	Ensemble recovery	—	$\mathcal{O}(K^3N^3 + DN^2K^2)$
Canonical-Moments form conversion	$\mathcal{O}(D^3)$	$\mathcal{O}(N^3 + N^2D)$	
Space Complexity	Covariance Matrix	$\mathcal{O}(D^2)$	$\mathcal{O}(ND)$
	Precision Matrix	$\mathcal{O}(D^2)$	$\mathcal{O}(ND)$

## J. Alternative linearisations and low rank decompositions

In response to a reviewer question, we investigate whether GEnBP is “just” a low-rank decomposition of the GaBP algorithm. We argue that it is not. Rather the relationship is that diagrammed by Fig. 10. Although the GEnBP and GaBP algorithms both use Gaussian approximations, they do not use the same Gaussian approximations. This is why we observe in Sec. 4 that GEnBP is able to surpass GaBP in accuracy and not just speed. We noted in app. C.3 that GaBP include not only a choice of Gaussian density family, which it shares with GEnBP, but also a particular means of approximating nonlinear factors which it does not. That apparently minor difference has large implications. We expand upon some of the differences and implications in this section.

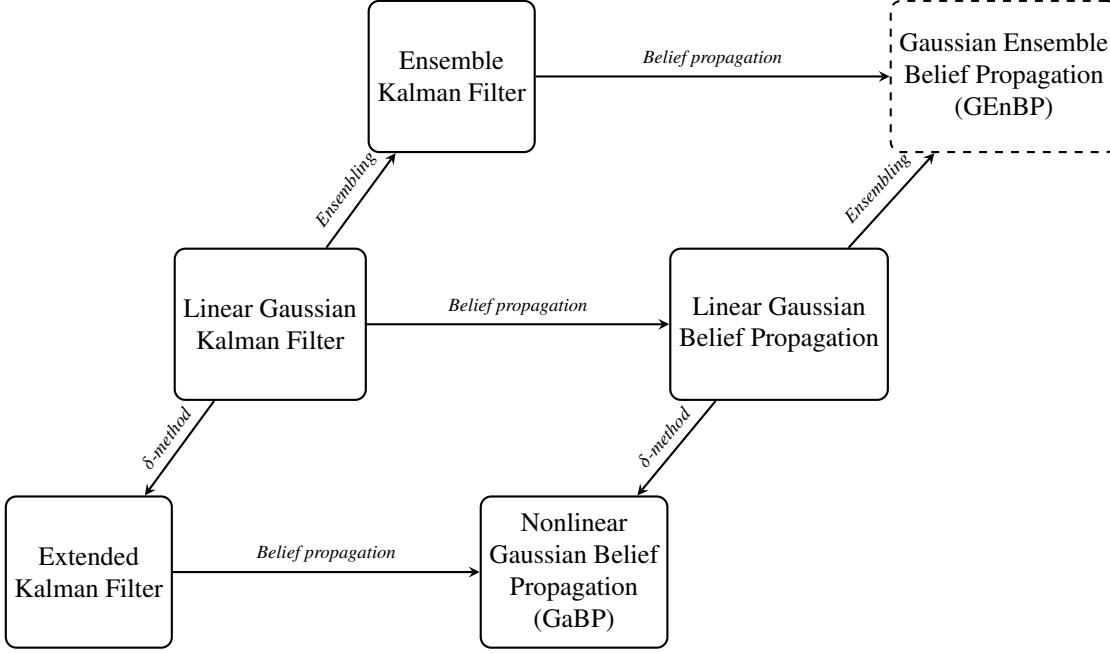


Figure 10: Relationship between GEnBP and GaBP.

Consider how the joint density of a factor  $\mathbf{x}_2 = \mathcal{P}(\mathbf{x}_1)$  to make the differences explicit. For the sake of simplicity, suppose  $D_1 = D_2 = D$ . Two alternatives for covariance estimation have been discussed in this work: GaBP uses propagation of errors,

$$\text{Var} \begin{bmatrix} \mathbf{x}_1 \\ \mathbf{x}_2 \end{bmatrix} \simeq \begin{bmatrix} \text{Var} \mathbf{x}_1 & J(\mathbf{m}_1) \text{Var} \mathbf{x}_1 \\ \text{Var} \mathbf{x}_1 J(\mathbf{m}_1)^\top & J(\mathbf{m}_1) \text{Var} \mathbf{x}_1 J^\top(\mathbf{m}_1) \end{bmatrix} \quad (96)$$

where  $J(x)$  is the jacobian matrix of  $\mathcal{P}$  at  $x$ . GEnBP, by contrast, uses the empirical estimate

$$\text{Var} \begin{bmatrix} \mathbf{x}_1 \\ \mathbf{x}_2 \end{bmatrix} \simeq \widehat{\text{Var}}_{\sigma^2 \mathbf{I}} \begin{bmatrix} x^{(1)} & \dots & x^{(N)} \\ \mathcal{P}(x^{(1)}) & \dots & \mathcal{P}(x^{(N)}) \end{bmatrix}. \quad (97)$$

As noted in App. I, the costs of (97) is greater than (96) both in time and space. There are two components to this cost:

Firstly, the cost of generating the ensemble (in GenBP) and the jacobians (in GaBP). In GEnBP, we need to generate  $N$  samples from the prior distribution, so the cost here scales as  $N$  in general. The cost of calculating the Jacobian for the GaBP depends on the function but in general is  $\mathcal{O}(D)$ .

Secondly, taking the matrix products in each of these covariance matrices. The matrix multiplication in (96) is  $\mathcal{O}(D^3)$ , since it involved the product of three  $D \times D$  matrices. The empirical covariance calculation in (97) is  $\mathcal{O}(DN)$ . We note that it *would* be  $\mathcal{O}(D^2N)$  if we were to calculate the full covariance matrix in GEnBP, but the central lesson of this paper is that we never need to calculate that product, and it suffices to calculate the deviance matrices.

It seems that at this stage, GEnBP dominates when  $N < D$ . We note that in the subsequent belief propagation the story is more complicated but that GEnBP has generally cheaper belief propagation steps (except where node degree is high). We might ask if GaBP can also benefit from these low-rank belief updates.

Suppose we wished to construct a 3rd option, a *low rank GaBP* (LRGaBP) which used a low-rank decomposition of the covariance matrix to conduct approximate GaBP. First, we would find rank  $N$  decomposition of the prior covariance  $\text{Var} \mathbf{x}_1 \approx \mathbf{L}\mathbf{L}^\top$ , with  $\mathbf{L} \in \mathbb{R}^{D \times N}$ , say by eigendecomposition, which is naively a  $D^3$  operation, or  $\mathcal{O}(D^2 \log N + N^2 D + N^3)$  by the method of (Halko et al., 2010, 6.1). The joint variance arising from the propagation-of-errors/ $\delta$  method (Dorfman,

1938) is

$$\text{Var} \begin{bmatrix} \mathbf{x}_1 \\ \mathbf{x}_2 \end{bmatrix} \simeq \begin{bmatrix} \text{Var} \mathbf{x}_1 & J(\mathbf{m}_1) \text{Var} \mathbf{x}_1 \\ \text{Var} \mathbf{x}_1 J(\mathbf{m}_1)^\top & J(\mathbf{m}_1) \text{Var} \mathbf{x}_1 J^\top(\mathbf{m}_1) \end{bmatrix} \quad (98)$$

$$= \begin{bmatrix} \text{LL}^\top & J(\mathbf{m}_1)\text{LL}^\top \\ \text{LL}^\top J(\mathbf{m}_1)^\top & J(\mathbf{m}_1)\text{LL}^\top J^\top(\mathbf{m}_1) \end{bmatrix} \quad (99)$$

$$= \begin{bmatrix} \text{L} \\ J(\mathbf{m}_1)\text{L} \end{bmatrix} \begin{bmatrix} \text{L} \\ J(\mathbf{m}_1)\text{L} \end{bmatrix}^\top \quad (100)$$

This is indeed a low-rank decomposition, amenable to similar tricks as the other low-rank tricks outlined in app. F. However, it is not computationally competitive.  $J$  is  $D \times D$  so the product costs  $\mathcal{O}(D^2N)$ , plus the  $\mathcal{O}(D)$  cost of calculating the Jacobian. We summarise the costs of this hypothetical LRGaBP step in table 3. Notably, while the precise relationship between the algorithms depends upon the exact problem structure, we should generally expect GEnBP to be more efficient than LRGaBP for high dimensional problems for a fixed  $N$ , since GEnBP is never worse than LRGaBP, and in many cases has a lower exponent in  $D$ .

Further, since LRGaBP is an approximation to GaBP, the accuracy of LRGaBP to be bounded above by the accuracy of GaBP. GEnBP, as a different approximation to the target estimand, has no such restriction.

Table 3: Computational Costs for Gaussian Belief Propagation, Ensemble Belief propagation, and the hypothetical Low Rank Gaussian Belief Propagation for node dimension  $D$ , ensemble size/component rank  $N$ .

Operation		GaBP	GEnBP	LRGaBP
Time Complexity	Simulation	$\mathcal{O}(1)$	$\mathcal{O}(N)$	$\mathcal{O}(1)$
	Error propagation	$\mathcal{O}(D^3)$	—	$\mathcal{O}(D^2N)$
	Jacobian calculation	$\mathcal{O}(D)$	—	$\mathcal{O}(D)$
	Covariance SVD	—	$\mathcal{O}(N^3 + N^2D)$	$\mathcal{O}(D^2 \log N + N^3 + N^2D)$
Space Complexity	Covariance Matrix	$\mathcal{O}(D^2)$	$\mathcal{O}(ND)$	$\mathcal{O}(ND + D^3)$
	Precision Matrix	$\mathcal{O}(D^2)$	$\mathcal{O}(ND)$	$\mathcal{O}(ND)$